

Transversal AND in Quantum Codes

Christine Li¹[0000–0001–6443–7090] and Lia Yeh²[0000–0003–2704–4057]

¹ Department of Computer Science, Columbia University, New York, USA
² Department of Computer Science and Technology, University of Cambridge,
Cambridge, UK
c14315@columbia.edu ly404@cam.ac.uk

Abstract. The AND gate is not reversible—on qubits. However, it *is* reversible on qutrits, making it a building block for efficient simulation of qubit computation using qutrits. We first observe that there are multiple two-qutrit Clifford+T unitaries that realize the AND gate with T-count 3, and its generalizations to n qubits with T-count $3n-3$. Our main result is the construction of a novel qutrit $[[6, 2, 2]]$ quantum error-correcting code with a transversal implementation of the AND gate. The key insight in our approach is that a symmetric T-depth one circuit decomposition — composed of a CX circuit, T and T dagger gates, followed by the CX circuit in reverse — of a given unitary can be interpreted as a CSS code. We can increase the code distance by augmenting the code circuit with additional stabilizers while preserving the logical gate. This results in a code with a “built-in” transversal implementation of the original unitary, which can be further concatenated to attain a $[[48, 2, 4]]$ code with the same transversal logical gate. Furthermore, we present several protocols for mixed qubit-qutrit codes which we call Qubit Subspace Codes, and for magic state distillation and injection.

Keywords: Quantum computing · Reversible computation · Quantum error correction · Qutrits · Exact circuit synthesis · ZX-calculus

1 Introduction

When computing with bits, the first gates we often learn are AND, OR, and NOT. When computing with qubits, one of the first concepts that we often learn is that the AND gate is not reversible. However, there *is* a reversible quantum AND gate—just not for qubits. We escape this restriction specific to qubits by working with the simplest possible extension—qutrits, i.e. three-level quantum systems instead of two-level.

Qutrits open up promising avenues due to many advantages, including more efficient algorithms, gates, and error-correcting codes. In many existing hardware architectures for quantum computers, qubits are a choice of two-dimensional subspace in what is natively a higher-dimensional setting. In choosing to actively encode and control quantum information in more levels, quantum computing with qudits is an active area of research in both theory and practice. Qudit computation has been experimentally demonstrated on systems such as nuclear magnetic resonance [25], nuclear spins [31], cold atoms [1], Rydberg atoms [77], linear

optics [41, 53], integrated photonics [17], trapped ion [40, 65], and superconducting [15, 33], with a recent demonstration of GKP qutrit error correction beyond break-even [9]. Qudit entanglement has demonstrated improved noise robustness compared to qubits [71], and leveraging qutrit states can improve fidelity of qubit operations [4, 10]. As the most well-studied qudit setting, qutrits can efficiently simulate qubit computation by reducing circuit depth or ancilla overhead, as shown for diagonal qubit unitaries [79], logarithmic-depth Toffoli [32], and binary AND gates [18], as well as factoring algorithms [7], probing lattice gauge theories [44, 56], variational quantum algorithms [16, 53], and unitary decomposition [53]. Qutrit operations can also be used to suppress leakage errors to the $|2\rangle$ state [57].

However, there is a gap between the qudit operations realizable on real-world hardware, and those that conceivably satisfy definitions of fault-tolerance; while definitions vary, the main principles are unchanged from what Gottesman laid out in 1997 [36]. A large reason for this is that pairwise two-level operations in a three-level quantum system, while natural to do in experimental implementations, does not embed naturally into qutrit stabilizer theory the way that it does for qubits. Another reason is that the qubit stabilizer fragment does not embed into the qutrit stabilizer fragment. Qutrit computation also offers a promising path to more efficient error-correcting codes, with better thresholds and yield rates in magic state distillation [12]. While prior work has explored various constructions of qutrit, prime-dimensional qudit, and composite-dimensional [38] codes, less attention has been given to finding qutrit codes with specific transversal logical operators, especially ones that are both non-Clifford and entangling. In this work, we take a logical operator-centric approach to code construction by reversing the typical procedure for designing stabilizer codes. Instead of deriving the logical operators from the fixed stabilizer set of a code, we start with a chosen logical operator, constructing the code around it by adding stabilizers. This work constitutes one of few efforts on improving qubit computation framed with respect to qutrit stabilizer computation, and to our knowledge is the first to construct qutrit stabilizer error-correcting codes expressly to this end.

Our approach to constructing qutrit codes with a binary AND gate logical operation centers on two components. The first is exact circuit synthesis, leveraging the known connection between exact circuit synthesis and error-correcting code constructions [11, 14]. The second is the ZX-calculus, by means of which a number of works have investigated new ways to represent and compile for quantum error-correcting codes. However, while more progress has been made on verifying and proving properties of codes and on compiling fault-tolerant circuits, there has been comparatively less use of ZX-calculus to construct specific new codes and protocols.

Combining the motivating ideas of (1) emulating qubit gates using qutrits and (2) constructing a QEC code around a particular logical operator, the central question we set out to answer in this work is:

How can we construct a non-trivial qutrit QEC code with a transversal implementation of a qubit logical gate?

2 Qubit and Qutrit Reversible Computation

For qutrits, the computational basis states are $|0\rangle$, $|1\rangle$, and $|2\rangle$. A normalized qutrit state can be written as $|\psi\rangle = \alpha|0\rangle + \beta|1\rangle + \gamma|2\rangle$, where $\alpha, \beta, \gamma \in \mathbb{C}$ and $|\alpha|^2 + |\beta|^2 + |\gamma|^2 = 1$. In a generalized d -dimensional system with computational basis states $|k\rangle$, where $k \in \mathbb{Z}_d$, the Pauli X and Z gates are defined as

$$X|k\rangle = |k+1 \pmod{d}\rangle, \quad Z|k\rangle = \omega^k|k\rangle$$

where $\omega = e^{\frac{2\pi i}{d}}$. For qutrits, $\omega = e^{\frac{2\pi i}{3}}$, and $\bar{\omega} := \omega^2 = \omega^{-1}$.

Definition 1 (Qutrit X gates). For qutrits, there are five non-trivial permutations of the computational basis states (all are Clifford): $X_{01}, X_{02}, X_{12}, X_{+1}, X_{-1}$. X_{+1} is the Pauli X gate for qutrits. $X_{-1} = X_{+1}^\dagger$, and $X^\dagger = X^2$. X_{01} acts as $|0\rangle \mapsto |1\rangle$, $|1\rangle \mapsto |0\rangle$, and $|2\rangle \mapsto |2\rangle$. X_{02} and X_{12} are defined analogously.

Definition 2 (Qutrit X basis). The X basis consists of the states $|+\rangle := \frac{1}{\sqrt{3}}(|0\rangle + |1\rangle + |2\rangle)$, $|\omega\rangle := \frac{1}{\sqrt{3}}(|0\rangle + \omega|1\rangle + \bar{\omega}|2\rangle)$, and $|\bar{\omega}\rangle := \frac{1}{\sqrt{3}}(|0\rangle + \bar{\omega}|1\rangle + \omega|2\rangle)$.

Definition 3 (Hadamard gate). The H gate is acts as $|0\rangle \mapsto |+\rangle$, $|1\rangle \mapsto |\omega\rangle$, $|2\rangle \mapsto |\bar{\omega}\rangle$. Note that unlike for qubits, $H \neq H^\dagger$, but $H^3 = H^\dagger$. $H^2 = X_{12}$ is the dualizer (also known as the antipode) for qutrits, and $H^4 = I$.

Definition 4 (Z phase gate). The Z phase gate is $Z(a, b) := \text{diag}(1, \omega^a, \omega^b)$, where $a, b \in \mathbb{R}$. It acts as $|k\rangle \mapsto \omega^k|k\rangle$ for $k \in \mathbb{Z}_3$. The Pauli Z gate is $Z(1, 2)$.

Definition 5 (X phase gate). The X phase gate is defined as $X(a, b) := HZ(a, b)H^\dagger$, where $a, b \in \mathbb{R}$. The Pauli X gate is $X(2, 1)$ and $X^\dagger = X(1, 2)$.

Definition 6 (T gate). The T gate is $T := Z(\frac{1}{3}, -\frac{1}{3}) = \text{diag}(1, e^{\frac{2\pi i}{9}}, e^{-\frac{2\pi i}{9}})$. Just as in qubits, the qutrit T gate is in the third level of the Clifford hierarchy.

For qutrit controlled gates, there are different notions of control. We use the following two in this work:

Definition 7 (Λ -controlled U). Given a qutrit unitary U , the Λ -controlled U gate (defined in [7]) acts as $|i\rangle|j\rangle \mapsto |i\rangle \otimes (U^i|j\rangle)$, for $i, j \in \{0, 1, 2\}$. An example of this is the two-qutrit CX gate, defined as $|i, j\rangle \mapsto |i, i+j \pmod{3}\rangle$. Unlike the CNOT gate for qubits, the CX gate is not self adjoint, but $(CX)^\dagger = (CX)^2$.

Definition 8 ($|0\rangle$ -controlled U gate). Given a qutrit unitary U , the $|0\rangle$ -controlled U is defined as $|0\rangle \otimes |\psi\rangle \mapsto |0\rangle \otimes U|\psi\rangle$, $|1\rangle \otimes |\psi\rangle \mapsto |1\rangle \otimes |\psi\rangle$, and $|2\rangle \otimes |\psi\rangle \mapsto |2\rangle \otimes |\psi\rangle$. The $|1\rangle$ - and $|2\rangle$ -controlled U gates are analogously defined. We can change the control value by conjugating the control qutrit by X or X^\dagger .

The CX gate is Clifford, while the $|0\rangle$ (or $|1\rangle$ or $|2\rangle$)-controlled gates are non-Clifford. Similar to the qubit case, the generators of the qutrit Clifford group are H, S, CX . Adding the non-Clifford T gate to the set, we get the Clifford+T gate set, which is universal [21] and admits an exact circuit synthesis algorithm [30].

Like in the qubit case, for any prime qudit dimension, X and Z generate the Pauli group, and the CX , S , and H gates generate the Clifford group. The $|0\rangle$ -controlled gate, or equivalently the CCX gate, when added to the H gate, generates the qudit Toffoli+Hadamard gate set [66]. [80] presents a comprehensive coverage of the Clifford+T and Toffoli+Hadamard gate sets for prime-dimensional qudits, and their representations in qudit ZX- and ZH-calculus.

2.1 Qubit and Qutrit ZX-calculus

The ZX-calculus is a graphical formalism for quantum computing in which linear maps are represented by diagrams built from basic generators called Z and X spiders, together with structural elements that allow wires to bend and cross [19]. Each diagram has a precise interpretation as a linear map: Sequential composition corresponds to matrix multiplication, parallel composition to tensor product, and the number of inputs and outputs determines whether the diagram represents a state, effect, map, or scalar. The calculus is equipped with rewrite rules that equate diagrams representing the same linear map. The qubit ZX-calculus is *sound*—any derivable equality reflects genuine equality of the underlying maps; *universal* for qubit linear maps—any qubit operation can be expressed as a ZX diagram; and *complete*—for any two equal diagrams, their equality can be proved entirely within the calculus [39].

We do not use the qubit ZX-calculus in this work; we use the qutrit ZX-calculus, first introduced in [64, 76]. All its wires represent a qutrit (three-level quantum information carrier) instead of a qubit (two-level). For qubits [3], qutrits [75], and qudits of any odd prime dimension [8, 61], the ZX-calculus is complete for the stabilizer or Clifford fragment of quantum computation.

The qutrit ZX-calculus is generated by the five diagrams

$$\left\{ \begin{array}{c} \vdots \\ \vdots \\ \text{---} \text{Z} \text{---} \\ \vdots \\ \vdots \end{array} , \begin{array}{c} \vdots \\ \vdots \\ \text{---} \text{X} \text{---} \\ \vdots \\ \vdots \end{array} , \text{---} \mathbb{1} \text{---} , \begin{array}{c} \text{---} \\ \diagdown \quad \diagup \\ \diagup \quad \diagdown \\ \text{---} \end{array} , \text{---} \right\} \quad (1)$$

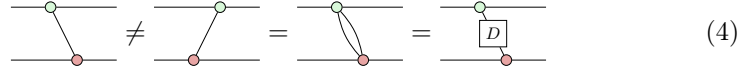
The interpretations of Z and X spiders as linear maps are

$$\left[\begin{array}{c} \vdots \\ \vdots \\ \text{---} \text{Z} \text{---} \\ \vdots \\ \vdots \end{array} \right]_m^n := |0\rangle^{\otimes m} \langle 0|^{\otimes n} + \omega^a |1\rangle^{\otimes m} \langle 1|^{\otimes n} + \omega^b |2\rangle^{\otimes m} \langle 2|^{\otimes n} \quad (2)$$

$$\left[\begin{array}{c} \vdots \\ \vdots \\ \text{---} \text{X} \text{---} \\ \vdots \\ \vdots \end{array} \right]_m^n := |+\rangle^{\otimes m} \langle +|^{\otimes n} + \omega^a |\omega\rangle^{\otimes m} \langle \omega|^{\otimes n} + \omega^b |\bar{\omega}\rangle^{\otimes m} \langle \bar{\omega}|^{\otimes n} \quad (3)$$

Note that when $m = n = 1$, the green Z spider corresponds to the Z phase gate $Z(a, b)$ and the X spider corresponds to the X phase gate $X(a, b)$. We use the non-flex-symmetric version of the qutrit ZX-calculus. This means that, unlike the qubit ZX-calculus, it is no longer the case that only connectivity matters. In

particular, CX is not equivalent to CX[†]:



In this work, we will mostly follow the notation from [74], where H is the yellow box labeled 1 and H^\dagger is the yellow box labeled 2. However, we use the horizontal orientation (left to right), rather than vertical (bottom to top), in keeping with common ZX-calculus usage in quantum error correction and circuit compilation works. We represent the dualizer (antipode), $X_{12} = H^2$, by a white box labeled D . The qutrit ZX-calculus rules are reprinted from [74] in Figure 1 in the appendix.

3 The AND Gate as a Quantum Circuit Primitive

3.1 Emulation: Qubit Computation using Qutrits

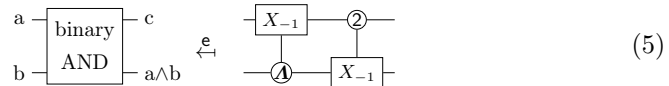
The first difficulty with developing a fault-tolerant theory of emulation is that qubit Cliffords are not a subgroup of qudit Cliffords. As a counterexample to show this: the $\text{diag}(1, -1, 1)$ gate is Clifford-equivalent (by conjugating by Pauli X) to the non-Clifford R gate.

We can also see that restricting a qutrit Clifford gate to its qubit subspace, is not necessarily a qubit Clifford operation. For example, the qutrit Pauli Z gate acts on the qubit subspace as $\text{diag}(1, \omega)$; $\omega = e^{i\frac{2\pi}{3}}$ is not an element of the ring which all qubit Clifford unitary matrices must be over [28].

It is impossible to implement binary AND gate using two qubits. However, it *is* possible to do so using two qutrits. By this we mean that we can construct two-qutrit circuit such that the behavior (i.e., truth table rows) of the first two levels $|0\rangle$ and $|1\rangle$ of the qutrit circuit matches that of the qubit binary AND gate. The behavior of the third level of the qutrit circuit is left unconstrained. The additional space afforded by the third level allows for the binary AND gate to be implemented unitarily.

Lemma 1. *The binary AND gate can be emulated by a two-qutrit Clifford+T unitary with T-count 3.*

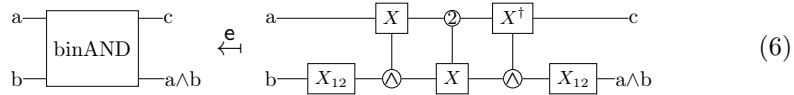
Proof. We will show that the below Clifford+T two-qutrit unitary emulates the binary AND gate:



Its cost is T-count 3 and Clifford CX-count 4. The cost calculation follows from the $|2\rangle$ -controlled X_{+1} gate comprising of 3 Clifford CX gates and 3 qutrit T gates [7]. Throughout this section, the letter e above the equals sign indicates it is an emulation. □

Interestingly, it outperforms the Toffoli gate, for which it is known that the optimal cost is 7 qubit T gates in the no-ancilla case [34], 6 qubit Clifford CX gates independent of ancillae count [69], and 5 two-qubit gates [83]. Even when ancillae and operations conditioned on measurement are permitted, the best known qubit Clifford+T decomposition of the Toffoli gate is 4 T gates [43].

A symmetric qutrit circuit which emulates the qutrit binary AND gate is:



We can check that both these circuits indeed emulate AND through Table 1. We

a	b	c	a^b
0	0	0	0
0	1	2	0
0	2	1	2
1	0	1	0
1	1	0	1
1	2	2	1
2	0	2	2
2	1	1	1
2	2	0	2

a	b	c	a^b
0	0	0	0
0	1	2	0
0	2	0	2
1	0	1	0
1	1	1	1
1	2	0	1
2	0	1	2
2	1	2	1
2	2	2	2

Table 1: Truth tables for AND emulations of Equations (5) (left) and (6) (right).

can change the control value of the $|2\rangle$ -controlled X by conjugating by Pauli X gates, and from controlled X to Z by conjugating by Hadamard gates.

Remark 1. Through fixing only the rows and columns corresponding to the binary AND gate (i.e., only rows where the inputs are 0 or 1, and the output column a^b), the remaining truth table entries shaded in Table 1 are a degree of freedom. We can therefore explore other circuit constructions so long as the AND action is preserved for binary inputs.

By applying the X_{01} gate (which emulates the binary NOT gate) to both inputs and to the AND'd output of Equation (5), in accordance with DeMorgan's law, the binary OR gate is emulated with the same T-count and Clifford CX-count. This leads us to:

Proposition 1. *All binary classical logic circuits can be emulated through exact synthesis in the qutrit Clifford+T gate set.*

Proof. AND, OR, NOT is a universal gate set for binary classical logic. As NOT can be emulated by a qutrit Clifford, the T-count is upper bounded by 3 times the total number of AND or OR gates. \square

We present in Table 2 a summary of the most efficient qutrit emulation of each binary or qubit gate that we calculated in Sections D.1 to D.3 of the appendix. There, we also give constructions for the qubit X, Z, S, CX and CZ gates, and $|+\rangle$ and $|-\rangle$ states, and prove why the qubit H gate cannot be exactly synthesized unitarily in qutrit Clifford+T. In addition to giving the non-Clifford gate count, for near-term applications we give the number of two-qutrit operations required, as on present-day qubit quantum computers, two-qubit operations are the dominant noise source. We also give the qutrit Clifford CX count where all other operations are single-qutrit Clifford+T gates.

Gate emulated	Non-Clifford gates	Clifford CX's	Two-qutrit gates
Binary AND	3 T	4	1
Binary OR	3 T	4	1
n -ary Binary AND [18]	$(3n - 3)$ T	$4n - 4$	$n - 1$
Qubit X (i.e. Binary NOT)	0	0	0
Qubit Z	1 R	0	0
Qubit CX [7]	6 T	8	1
Qubit CZ [79]	3 R	3	1
Qubit CCX [7]	12 T	15	3
Qubit CCZ [79]	3 R	5	3
Qubit C^n X, linear depth	$6n$ T	$6n + 3$	$2n - 1$
Qubit C^n Z, linear depth	$(6n - 12)$ T + 3 R	$6n - 7$	$2n - 1$
Qubit C^n X, log depth [18]	$6n$ T	$8n$	$2n - 1$
Qubit C^n Z, log depth	$(6n - 12)$ T + 3 R	$8n - 5$	$2n - 1$
Qubit C^n X, log depth [32]	$27n + 12$ T	$64n + 13$	$3.5n + 1$

Table 2: Resource counts for binary and qubit emulations unitarily without ancillae by qutrit gates. For decompositions in the literature given in terms of ternary classical reversible gates, these are computed by substituting the best known decompositions gate-wise, optimizing where possible. The $|+\rangle$, $|0\rangle$, and S gate counts are omitted because they are probabilistic constructions.

These counts are straightforward, but they show that the asymptotic non-Clifford gate counts of n -ary AND and qubit C^n X in ancilla-free qutrit Clifford+T, outperform the best known constant-ancilla qubit decomposition according to [23]: [46] having T-count $8n - 12$. The n -ary AND moreover has lower T-count than the best known $O(n)$ ancilla qubit decompositions [27] having T-count $4n - 6$ and T-depth $\lceil \log_2 \frac{n}{3} \rceil + 2$ [58]. More importantly, these qutrit decompositions are unitary, meaning that unlike the best-known qubit decompositions, they do not require feedforward of measurement outcomes to classically control any of their gates. We remark the possibility that similar AND gate-based techniques that halved T-count of multiple-controlled Toffolis and other binary computations in the qubit case [26], could be used to improve the depth of these qutrit constructions by allowing ancillae, for instance by preceding n -ary AND by a depth-1 layer of n CX gates to n ancilla in the $|0\rangle$ state.

Considering evidence that qudit emulation of individual multi-qubit gates in qubit circuits is of limited effectiveness [53], instead of resynthesizing gates in qubit circuits on an individual basis, a more promising approach would be to generalize the above approach for the AND gate, to binary classical reversible functions emulated with ternary classical reversible functions. Explicit constructions exist for any qudit dimension d , of any d -ary classical reversible function $f : \mathbb{Z}_d^n \rightarrow \mathbb{Z}_d^n$ on n dits by a circuit of $O(d^n n)$ $|0\rangle$ -controlled X gates and $O(n)$ ancillae prepared in the $|0\rangle$ state ([66, 84], building on [82]), thus putting the T-count for any odd prime d at $O(d^n n)$. This puts the best known upper and lower bounds at a log factor separation: For any qudit dimension d , there exist d -ary classical reversible functions $f : \mathbb{Z}_d^n \rightarrow \mathbb{Z}_d^n$ that require at least $O(nd^n / \log n)$ single-qudit and two-qudit gates to construct, even when allowed $\Omega(n)$ ancillae [66]. More generally, techniques to compress qubit circuits using qudit decompositions [53] or using mixed-dimensional quantum systems by clustering weighted graphs [54] can also be leveraged—from there, the difficult next steps are to decompose into conceivably fault-tolerant gates, or to build error-correcting codes around them as we will next do.

3.2 A T-depth 1 Symmetric Circuit as a $[[3, 2, 1]]$ Qutrit Code

As noted in Remark 1 there are many qutrit circuits that emulate the binary AND gate. From prioritizing those with low T-count, but more importantly, are symmetric and T-depth one, we found:

$$(7)$$

where we can apply the symmetric T-depth one decomposition of the $|0\rangle$ -controlled Z gate from Figure 7 of [7]. Therefore, the full Clifford+T symmetric T-depth one qutrit circuit decomposition of the qubit binary AND gate is given by

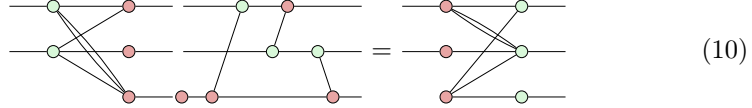
$$(8)$$

In ZX-calculus, this is equivalent to

$$(9)$$

To see how this forms the encoder (and decoder) of a QEC code, we can use ZX-calculus to transform the first half of circuit into the Generalized Parity

Form (GPF). From this we can directly “read off” the Z and X-type logical basis operators and stabilizer generators. Notice that this circuit contains other gates besides CNOTs, which means that the corresponding code is not a CSS code. However, for the purposes of finding the stabilizer generators and logical operators and determining code distance, it is sufficient to focus on just the CSS portion of the circuit, which is composed of the inner CX gates [48]. Therefore, from the CNOT encoder portion, we get the encoder in Z-X (left) and X-Z (right) normal forms [42, 48, 49]:

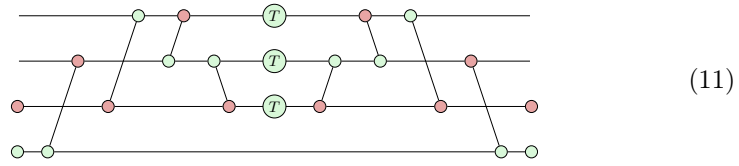


From the connectivity of the Z-X form of the encoder, the X-type logical operators are $\bar{X}_1 = X_1X_3^2$ and $\bar{X}_2 = X_1X_2X_3$. There are no X-type stabilizers. From the X-Z form of the encoder, the Z-type logical operators and stabilizer generators are $\bar{Z}_1 = Z_1Z_2^2$ and $\bar{Z}_2 = Z_2$, and $S_1^Z = Z_1Z_2Z_3$. We can observe the code distance is 1, since there is a logical Z-type operator of weight 1.

4 Reconstructing the Code at Higher Distance

To increase the code distance, we would need to add X-type stabilizers, while ensuring that the distance stays the same. We take inspiration from an observation about the qubit $[[8, 3, 2]]$ code construction from [11], which we deconstruct in the ZX-calculus in Sections B.1 and B.2 of the appendix.

In an attempt to reproduce how to construct the $[[8, 3, 2]]$ code by adding an X-type stabilizer to all physical qubits of a $[[7, 3, 1]]$ code with transversal CCZ, we add an X-type stabilizer that checks all qubits: $S_1^X = X_1X_2X_3$. Adding to our earlier encoder, which we conjugate $T^{\otimes 3}$ by, and after applying ZX rewrite rules to “push” the stabilizer outside of the encoder/decoder, we obtain the following symmetric circuit:



Since the inner portion of the circuit is still the same as before adding the stabilizer, this is the $|0\rangle$ -controlled Z gate with a CX gate applied from an extra ancilla (which is initialized and postselected to $|+\rangle$) to the second data qubit on either sides. Therefore, the equivalent circuit is



However, we can see that the logical gate corresponding to this circuit is no longer the same.

4.2 Deriving the Code as a Symmetric, T-depth One Circuit

In order to determine the corresponding QEC code, our approach is to solve for a symmetric, T-depth one synthesis of the circuit. We can rewrite the circuit in its symmetric form using *phase gadgets*—symmetric multi-qubit interactions native to many hardware architectures [59, 60, 68] and useful for optimizing quantum circuits [6, 20, 78].

First, we will find the phase gadgets representation of the $|0\rangle$ -controlled Z and Z^\dagger gates. Then, we will find the combined phase gadgets form. From this, we can obtain a T-depth one symmetric form of the circuit.

We begin with the symmetric circuit for $|0\rangle$ -controlled from [7]. To rewrite this in phase gadgets form, we will need to use Eq (6) of [79] (which can be derived using spider fusion, bialgebra rule, and dualizing). Therefore,

(17)

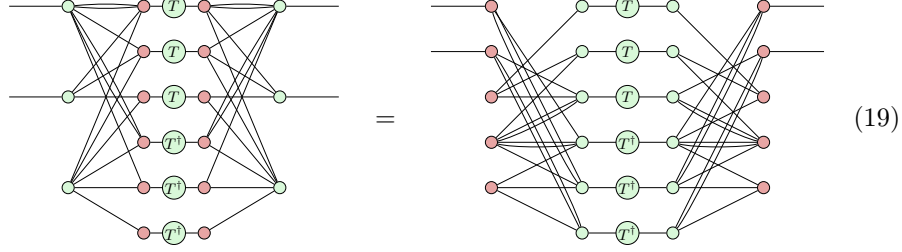
(18)

To find the phase gadget form of its adjoint, $|0\rangle$ -controlled Z^\dagger , we take the adjoint of the phase gadget diagram that we just found, by taking its horizontally reflection and negating the phases. Applying dualizers to all wires surrounding the red X spiders flips back the direction of the phase gadgets, so we end up with the same diagram for $|0\rangle$ -controlled Z^\dagger except with T^\dagger instead of T phases. Therefore, we can replace the $|0\rangle$ -controlled Z and Z^\dagger gates with their respective phase gadget representation, then rewrite and apply the rule from [79] to obtain a combined phase gadgets form.

4.3 Finding the Stabilizers and Logical Operators

From the combined phase gadgets diagram, we can obtain a symmetric circuit by reading off the connectivity for each of the phase gadgets' spiders. This is because the above diagram corresponds to phase polynomials based on sum over paths for each of the phase gadgets, which can equivalently be expressed in a symmetric form that computes a parity map on the left then uncomputes on the right, which is also equivalent to a CNOT circuit with phase gates and pre/postselection (see Chapter 7.1 of [49]). Thus, from the combined phase gadget diagram above, we

obtain the following symmetric forms:



The left portion of the diagrams represents the encoder maps, and symmetrically, the right portion the decoder map. In the left hand side diagram, the encoder is in the Z-X form [48]. From this, we can read off the X-type stabilizers and logical operators. The diagram on the right hand side is the corresponding X-Z encoder, obtained by applying bialgebra, dual, and fusion rewrite rules. From the X-Z form, we can read off the Z-type stabilizers and logical operators. Thus, for this inner CSS code (which implements the $|0\rangle$ -controlled Z), the two equivalent encoder maps, along with the corresponding stabilizer generators and logical operators are:

$$\begin{aligned}
 \bar{X}_1 &= X_1^2 X_2 X_4^2 X_5 \\
 \bar{X}_2 &= X_1 X_2 X_3 \\
 S_{X1} &= X_1 X_2 X_3 X_4 X_5 X_6
 \end{aligned}
 \quad
 \begin{aligned}
 &= \\
 &
 \end{aligned}
 \quad
 \begin{aligned}
 \bar{Z}_1 &= Z_4 Z_5^2 \\
 \bar{Z}_2 &= Z_3 Z_6^2 \\
 S_{Z1} &= Z_1 Z_2 Z_3 \\
 S_{Z2} &= Z_2 Z_3^2 Z_4^2 Z_5 \\
 S_{Z3} &= Z_4 Z_5 Z_6
 \end{aligned}
 \tag{20}$$

Recall (see Eq. 9) that the overall symmetric T-depth 1 circuit for AND gate consists of outer Clifford gates in addition to the inner CX circuit. The encoders above are for the CSS code corresponding to this inner CX circuit.

By pushing logical X and Z spiders through the full encoder, we obtain the following logical operators for the “overall” code implementing transversal AND:

$$\begin{aligned}
 \bar{X}_1 &= X_1^2 X_2 X_4^2 X_5 & \bar{Z}_1 &= X_1 X_2 X_3 Z_4 Z_5^2 \\
 \bar{X}_2 &= X_1 X_2^2 Z_3^2 X_4 X_5^2 Z_6 & \bar{Z}_2 &= X_1 X_2 X_3
 \end{aligned}
 \tag{21}$$

We verify that the code distance is 2 by checking the minimum weight of all possible logical operators (such as by multiplying each logical operator with all possible linear combinations of the stabilizers, for this small code).

We will use E_{pf} to refer to the inner CSS encoder in Eq. 20 (comprised of phase-free “pf” spiders) for the CSS code implementing the $|0\rangle$ -controlled Z. We will use E_{AND} to refer to the full encoder (consisting of outer Clifford gates and E_{pf}) for the $[[6, 2, 2]]$ qutrit code implementing transversal AND.

4.4 Getting to Distance 4 Through Code Concatenation

We remark that our $[[6, 2, 2]]$ qutrit code with a transversal AND gate (implemented by 3 T and 3 T^\dagger gates), can be concatenated as the outer code with the inner $[[8, 1, 2]]$ qutrit CSS code with transversal T gate from [13]. As both are qutrit CSS codes and the inner CSS code's X and Z logical operators are implemented by physical X's and Z's respectively, the resulting code distance is the product of that of the inner and outer codes³: $[[48, 2, 4]]$, with transversal AND gate implemented by 24 T and 24 T^\dagger gates.

5 Qubit Subspace Codes

In this section, we will introduce Qubit Subspace Projection as a logical operation in qutrit codes. In addition, depending on how these results are utilized, these can be viewed from the perspectives of gauge fixing of subsystem codes, and as adding additional stabilizers to construct mixed qubit-qutrit codes which we call Qubit Subspace Codes. We begin by deriving for the qutrit setting, the physical action of logical ZX diagrams for CSS codes in Section A.1 of the appendix.

5.1 Logical Qubit, Physical Qutrits

We describe how to derive a quantum code that encodes a logical qubit ($k = 1$) using $n = 6$ physical qutrits. While we suspect this first Qubit Subspace Code is of more limited use than the one in the next subsection, this also serves as a simpler demonstration of code construction techniques:

Begin with E_{pf} , the encoder for the $[[6, 2, 2]]$ inner qutrit CSS code implementing $|0\rangle$ -controlled Z (henceforth denoted ZCZ for short). Fix the bottom logical qutrit to $|0\rangle_L$, apply logical X to the top qutrit (to the left of the encoder), measure the bottom logical qutrit in the X basis, and check if it is $\langle + |_L$ using Steane error correction [72] on a $|0\rangle_L |+\rangle_L$ resource state. This procedure, presented in more detail in Section C.4 of the appendix, uses gauge fixing to enable a logical operation, by projecting the top logical qutrit into the qubit subspace.

5.2 Qubit Subspace Projection

Now, we will show how to obtain a code with $k = 2$ logical qubits and $n = 6$ physical qutrits that has the same stabilizers as that of E_{AND} , but has two additional stabilizers which project the two logical qutrits into the qubit subspace.

The following logical circuit implements a projection of the top qutrit into the $|0\rangle$ and $|1\rangle$ subspace. We call this the qubit subspace projection (SP) gadget.

³ This is a well-known result [37], deducible by presuming that any logical error can occur if at least d_{outer} logical qubits of the inner CSS code experienced errors, each of which had to have experienced at least d_{inner} physical errors.

to C.4 of the appendix.

(25)

There we also prove correctness of magic state distillation and deterministic injection of the AND gate for qutrit CSS codes. The correction is a Clifford unitary where all but one gate—the $Z(2b, 2b)$ gate—are Pauli or CX gates, and hence transversally implementable on CSS codes [35].

7 Conclusion

In this work, we demonstrated that moving to qutrit systems enables an efficient unitary realization of the classical binary AND gate within the Clifford+T framework, and we developed explicit low-T-count constructions such as generalizing to multi-input AND. By reinterpreting symmetric compute-phase-uncompute decompositions as encoding and decoding circuits, we showed how to design qutrit stabilizer codes that admit transversal non-Clifford implementations of logical AND, including a $[[6, 2, 2]]$ code and a concatenated extension with increased distance. We further introduced mixed-dimensional subspace constructions and protocols for magic state distillation and deterministic injection compatible with qutrit CSS codes. Together, these results illustrate how higher-dimensional and mixed-dimensional code design can expand the landscape of fault-tolerant logical gates beyond qubit-based constraints, and motivate further investigation of their practical performance and scalability.

A natural question to investigate through in-depth comparative study would be how theorized qutrit codes perform under different noise models and hardware constraints. These could utilize recent software libraries for qudit computation such as [45, 55], in order to benchmark via numerical simulation against qubit codes with transversal CCZ gates, such as the $[[8, 3, 2]]$ color code (implemented by physical T and T^\dagger gates) or the $[[27, 3, 3]]$ code of [51] (implemented by a depth-2 physical CCZ circuit).

The other promising direction is to continue pushing the theory of higher-dimensional QEC code constructions. For discovering more codes and dynamic QEC protocols for a fixed qudit dimension, we can leverage normal forms such as for qutrit Clifford circuits [52], for qubit Clifford isometries [47, 81] (which we expect admit straightforward generalization to prime-dimensional qudits due to [61, 66]), and qutrit Clifford+T circuits [30].

Acknowledgments. Thank you to Nadish de Silva for explaining the approach for efficient multi-qudit gate teleportation described in [70]. We would like to thank Noah Goss, Matt McEwen, Costin Iancu, and Ed Younis for discussions about useful circuit

constructions for three-level quantum systems. We would like to thank Sarah Meng Li and Jacky (Jiaxin) Huang for the collaboration on pushing through the encoder and gauge fixing in [42] that greatly informed this work. We would like to thank Aleks Kissinger for discussions on the transversal CCZ of $[[8, 3, 2]]$ code. LY would like to thank the Google PhD Fellowship, and the Tencent Post-Doctoral Research Fellowship at the University of Cambridge, for funding.

References

1. Anderson, B.E., Sosa-Martinez, H., Riofrío, C.A., Deutsch, I.H., Jessen, P.S.: Accurate and robust unitary transformations of a high-dimensional quantum system. *Phys. Rev. Lett.* **114**, 240401 (Jun 2015). <https://doi.org/10.1103/PhysRevLett.114.240401>, <https://link.aps.org/doi/10.1103/PhysRevLett.114.240401>
2. Anwar, H., Campbell, E.T., Browne, D.E.: Qutrit magic state distillation. *New Journal of Physics* **14**(6), 063006 (Jun 2012). <https://doi.org/10.1088/1367-2630/14/6/063006>, <https://iopscience.iop.org/article/10.1088/1367-2630/14/6/063006>
3. Backens, M.: The zx-calculus is complete for stabilizer quantum mechanics. *New Journal of Physics* **16**(9), 093021 (Sep 2014). <https://doi.org/10.1088/1367-2630/16/9/093021>, <http://dx.doi.org/10.1088/1367-2630/16/9/093021>
4. Bækkegaard, T., Kristensen, L.B., Loft, N.J.S., Andersen, C.K., Petrosyan, D., Zinner, N.T.: Realization of efficient quantum gates with a superconducting qubit-qutrit circuit. *Scientific Reports* **9**(1), 13389 (Sep 2019). <https://doi.org/10.1038/s41598-019-49657-1>, <https://doi.org/10.1038/s41598-019-49657-1>
5. Baker, J.M., Duckering, C., Gokhale, P., Brown, N.C., Brown, K.R., Chong, F.T.: Improved quantum circuits via intermediate qutrits. *ACM Transactions on Quantum Computing* **1**(1), 1–25 (2020)
6. de Beaudrap, N., Bian, X., Wang, Q.: Techniques to Reduce $\pi/4$ -Parity-Phase Circuits, Motivated by the ZX Calculus. *Electronic Proceedings in Theoretical Computer Science* **318**, 131–149 (may 2020). <https://doi.org/10.4204/eptcs.318.9>
7. Bocharov, A., Roetteler, M., Svore, K.M.: Factoring with qutrits: Shor’s algorithm on ternary and metaplectic quantum architectures. *Physical Review A* **96**(1), 012306 (Jul 2017). <https://doi.org/10.1103/PhysRevA.96.012306>, <http://link.aps.org/doi/10.1103/PhysRevA.96.012306>
8. Booth, R.I., Carette, T.: Complete zx-calculi for the stabiliser fragment in odd prime dimensions. vol. 241, pp. 24:1–24:15. Schloss Dagstuhl – Leibniz-Zentrum für Informatik (2022). <https://doi.org/10.4230/LIPICS.MFCS.2022.24>, <https://drops.dagstuhl.de/entities/document/10.4230/LIPICS.MFCS.2022.24>
9. Brock, B.L., Singh, S., Eickbusch, A., Sivak, V.V., Ding, A.Z., Frunzio, L., Girvin, S.M., Devoret, M.H.: Quantum error correction of qudits beyond break-even. *Nature* **641**(8063), 612–618 (May 2025). <https://doi.org/10.1038/s41586-025-08899-y>, <https://www.nature.com/articles/s41586-025-08899-y>
10. Brown, T., Doucet, E., Ristè, D., Ribeill, G., Cicak, K., Aumentado, J., Simmonds, R., Govia, L., Kamal, A., Ranzani, L.: Trade off-free entanglement stabilization in a superconducting qutrit-qubit system. *Nature Communications* **13**(1), 3994 (Jul 2022). <https://doi.org/10.1038/s41467-022-31638-0>, <https://doi.org/10.1038/s41467-022-31638-0>

11. Campbell, E.T.: The smallest interesting colour code (Sep 2016), <https://earlrcampbell.com/2016/09/26/the-smallest-interesting-colour-code/>
12. Campbell, E.T., Anwar, H., Browne, D.E.: Magic-State Distillation in All Prime Dimensions Using Quantum Reed-Muller Codes. *Physical Review X* **2**(4), 041021 (Dec 2012). <https://doi.org/10.1103/PhysRevX.2.041021>, <https://link.aps.org/doi/10.1103/PhysRevX.2.041021>
13. Campbell, E.T., Anwar, H., Browne, D.E.: Magic-state distillation in all prime dimensions using quantum reed-muller codes. *Phys. Rev. X* **2**, 041021 (Dec 2012). <https://doi.org/10.1103/PhysRevX.2.041021>, <https://link.aps.org/doi/10.1103/PhysRevX.2.041021>
14. Campbell, E.T., Howard, M.: Unified framework for magic state distillation and multiqubit gate synthesis with reduced resource cost. *Physical Review A* **95**(2) (Feb 2017). <https://doi.org/10.1103/physreva.95.022316>, <http://dx.doi.org/10.1103/PhysRevA.95.022316>
15. Cao, S., Bakr, M., Campanaro, G., Fasciati, S.D., Wills, J., Lall, D., Shteynas, B., Chidambaram, V., Rungger, I., Leek, P.: Emulating two qubits with a four-level transmon qudit for variational quantum algorithms. *Quantum Science and Technology* **9**(3), 035003 (apr 2024). <https://doi.org/10.1088/2058-9565/ad37d4>, <https://doi.org/10.1088/2058-9565/ad37d4>
16. Cao, S., Bakr, M., Campanaro, G., Fasciati, S.D., Wills, J., Lall, D., Shteynas, B., Chidambaram, V., Rungger, I., Leek, P.: Emulating two qubits with a four-level transmon qudit for variational quantum algorithms. *Quantum Science and Technology* **9**(3), 035003 (apr 2024). <https://doi.org/10.1088/2058-9565/ad37d4>, <https://doi.org/10.1088/2058-9565/ad37d4>
17. Chi, Y., Huang, J., Zhang, Z., Mao, J., Zhou, Z., Chen, X., Zhai, C., Bao, J., Dai, T., Yuan, H., Zhang, M., Dai, D., Tang, B., Yang, Y., Li, Z., Ding, Y., Oxenl we, L.K., Thompson, M.G., O'Brien, J.L., Li, Y., Gong, Q., Wang, J.: A programmable qudit-based quantum processor. *Nature Communications* **13**(1), 1166 (Mar 2022). <https://doi.org/10.1038/s41467-022-28767-x>, <https://doi.org/10.1038/s41467-022-28767-x>
18. Chu, J., He, X., Zhou, Y., Yuan, J., Zhang, L., Guo, Q., Hai, Y., Han, Z., Hu, C.K., Huang, W., Jia, H., Jiao, D., Li, S., Liu, Y., Ni, Z., Nie, L., Pan, X., Qiu, J., Wei, W., Nuerbolati, W., Yang, Z., Zhang, J., Zhang, Z., Zou, W., Chen, Y., Deng, X., Deng, X., Hu, L., Li, J., Liu, S., Lu, Y., Niu, J., Tan, D., Xu, Y., Yan, T., Zhong, Y., Yan, F., Sun, X., Yu, D.: Scalable algorithm simplification using quantum AND logic. *Nature Physics* **19**(1), 126–131 (Jan 2023). <https://doi.org/10.1038/s41567-022-01813-7>, <https://www.nature.com/articles/s41567-022-01813-7>
19. Coecke, B., Duncan, R.: Interacting quantum observables: categorical algebra and diagrammatics. *New Journal of Physics* **13**(4), 043016 (Apr 2011). <https://doi.org/10.1088/1367-2630/13/4/043016>, <http://dx.doi.org/10.1088/1367-2630/13/4/043016>
20. Cowtan, A., Dilkes, S., Duncan, R., Simmons, W., Sivarajah, S.: Phase Gadget Synthesis for Shallow Circuits. In: Coecke, B., Leifer, M. (eds.) *Proceedings 16th International Conference on Quantum Physics and Logic*, Chapman University, Orange, CA, USA., 10-14 June 2019. *Electronic Proceedings in Theoretical Computer Science*, vol. 318, pp. 213–228. Open Publishing Association (2020). <https://doi.org/10.4204/EPTCS.318.13>
21. Cui, S.X., Wang, Z.: Universal quantum computation with metaplectic anyons. *Journal of Mathematical Physics* **56**(3), 032202 (03 2015). <https://doi.org/10.1063/1.4914941>

22. Dawkins, H., Howard, M.: Qutrit magic state distillation tight in some directions. *Phys. Rev. Lett.* **115**, 030501 (Jul 2015). <https://doi.org/10.1103/PhysRevLett.115.030501>, <https://link.aps.org/doi/10.1103/PhysRevLett.115.030501>
23. Dutta, S., Wang, S., Baksi, A., Chattopadhyay, A., Maitra, S.: On exact space-depth trade-offs in multi-controlled toffoli decomposition (2025), <https://arxiv.org/abs/2502.01433>
24. Garvie, L., Duncan, R.: Verifying the smallest interesting colour code with quantum. *Electronic Proceedings in Theoretical Computer Science* **266**, 147–163 (Feb 2018). <https://doi.org/10.4204/eptcs.266.10>, <http://dx.doi.org/10.4204/EPTCS.266.10>
25. Gedik, Z., Silva, I.A., Çakmak, B., Karpat, G., Vidoto, E.L.G., Soares-Pinto, D.O., deAzevedo, E.R., Fanchini, F.F.: Computational speed-up with a single qudit. *Scientific Reports* **5**(1), 14671 (Oct 2015). <https://doi.org/10.1038/srep14671>, <https://doi.org/10.1038/srep14671>
26. Gidney, C.: Halving the cost of quantum addition. *Quantum* **2**, 74 (Jun 2018). <https://doi.org/10.22331/q-2018-06-18-74>, <http://dx.doi.org/10.22331/q-2018-06-18-74>
27. Gidney, C., Jones, N.C.: A cccz gate performed with 6 t gates (2021), <https://arxiv.org/abs/2106.11513>
28. Giles, B., Selinger, P.: Exact synthesis of multiqubit clifford+t circuits. *Physical Review A* **87**(3) (Mar 2013). <https://doi.org/10.1103/physreva.87.032332>, <http://dx.doi.org/10.1103/PhysRevA.87.032332>
29. Glaudell, A.N., Ross, N.J., Taylor, J.M.: Canonical forms for single-qutrit clifford+t operators. *Annals of Physics* **406**, 54–70 (Jul 2019). <https://doi.org/10.1016/j.aop.2019.04.001>
30. Glaudell, A.N., Ross, N.J., Wetering, J.v.d., Yeh, L.: Exact Synthesis of Multiqutrit Clifford-Cyclotomic Circuits (Aug 2024), <http://arxiv.org/abs/2405.08136>
31. Godfrin, C., Ferhat, A., Ballou, R., Klyatskaya, S., Ruben, M., Wernsdorfer, W., Balestro, F.: Operating quantum states in single magnetic molecules: Implementation of grover’s quantum algorithm. *Phys. Rev. Lett.* **119**, 187702 (Nov 2017). <https://doi.org/10.1103/PhysRevLett.119.187702>, <https://link.aps.org/doi/10.1103/PhysRevLett.119.187702>
32. Gokhale, P., Baker, J.M., Duckering, C., Brown, N.C., Brown, K.R., Chong, F.T.: Asymptotic improvements to quantum circuits via qutrits. In: *Proceedings of the 46th International Symposium on Computer Architecture*. pp. 554–566. ACM, Phoenix Arizona (Jun 2019). <https://doi.org/10.1145/3307650.3322253>, <https://dl.acm.org/doi/10.1145/3307650.3322253>
33. Goss, N., Morvan, A., Marinelli, B., Mitchell, B.K., Nguyen, L.B., Naik, R.K., Chen, L., Jünger, C., Kreikebaum, J.M., Santiago, D.I., Wallman, J.J., Siddiqi, I.: High-fidelity qutrit entangling gates for superconducting circuits. *Nature Communications* **13**(1), 7481 (Dec 2022). <https://doi.org/10.1038/s41467-022-34851-z>, <https://www.nature.com/articles/s41467-022-34851-z>
34. Gosset, D., Kliuchnikov, V., Mosca, M., Russo, V.: An algorithm for the t-count. *Quantum Info. Comput.* **14**(15–16), 1261–1276 (Nov 2014)
35. Gottesman, D.: Stabilizer codes and quantum error correction. Ph.D. thesis, California Institute of Technology (1997). <https://doi.org/10.48550/arXiv.quant-ph/9705052>
36. Gottesman, D.: Theory of fault-tolerant quantum computation. *Physical Review A* **57**(1), 127–137 (Jan 1998). <https://doi.org/10.1103/physreva.57.127>, <http://dx.doi.org/10.1103/PhysRevA.57.127>

37. Gottesman, D.: 9.1 Concatenated Codes, p. 141–144. Textbook manuscript preprint (2024), <http://www.cs.umd.edu/~dgottesm/QECCbook-2024.pdf>
38. Gunderman, L.G.: Beyond integral-domain stabilizer codes. *Phys. Rev. A* **112**, 062430 (Dec 2025). <https://doi.org/10.1103/4y6f-xx6s>, <https://link.aps.org/doi/10.1103/4y6f-xx6s>
39. Hadzihasanovic, A., Ng, K.F., Wang, Q.: Two complete axiomatisations of pure-state qubit quantum computing. In: Proceedings of the 33rd Annual ACM/IEEE Symposium on Logic in Computer Science. p. 502–511. LICS '18, Association for Computing Machinery, New York, NY, USA (2018). <https://doi.org/10.1145/3209108.3209128>, <https://doi.org/10.1145/3209108.3209128>
40. Hrmo, P., Wilhelm, B., Gerster, L., van Mourik, M.W., Huber, M., Blatt, R., Schindler, P., Monz, T., Ringbauer, M.: Native qudit entanglement in a trapped ion quantum processor. *Nature Communications* **14**(1), 2242 (Apr 2023). <https://doi.org/10.1038/s41467-023-37375-2>, <https://doi.org/10.1038/s41467-023-37375-2>
41. Hu, X.M., Guo, Y., Liu, B.H., Huang, Y.F., Li, C.F., Guo, G.C.: Beating the channel capacity limit for superdense coding with entangled ququarts. *Science Advances* **4**(7), eaat9304 (2018). <https://doi.org/10.1126/sciadv.aat9304>, <https://www.science.org/doi/abs/10.1126/sciadv.aat9304>
42. Huang, J., Li, S.M., Yeh, L., Kissinger, A., Mosca, M., Vasmer, M.: Graphical css code transformation using zx calculus. *Electronic Proceedings in Theoretical Computer Science* **384**, 1–19 (Aug 2023). <https://doi.org/10.4204/eptcs.384.1>, <http://dx.doi.org/10.4204/EPTCS.384.1>
43. Jones, C.: Low-overhead constructions for the fault-tolerant toffoli gate. *Phys. Rev. A* **87**, 022328 (Feb 2013). <https://doi.org/10.1103/PhysRevA.87.022328>, <https://link.aps.org/doi/10.1103/PhysRevA.87.022328>
44. Joshi, R., Louw, J.C., Meth, M., Osborne, J.J., Mato, K., Su, G.X., Ringbauer, M., Halimeh, J.C.: Probing hadron scattering in lattice gauge theories on qudit quantum computers (2025), <https://arxiv.org/abs/2507.12614>
45. Kabir, A., Nguyen, S., Ghosh, S., Kiran, T., Kim, I.H., Huang, Y.: Sdim: A qudit stabilizer simulator (2025), <https://arxiv.org/abs/2511.12777>
46. Khattar, T., Gidney, C.: Rise of conditionally clean ancillae for efficient quantum circuit constructions. *Quantum* **9**, 1752 (May 2025). <https://doi.org/10.22331/q-2025-05-21-1752>, <http://dx.doi.org/10.22331/q-2025-05-21-1752>
47. Khesin, A.B., Lu, J.Z., Shor, P.W.: Universal graph representation of stabilizer codes. *PRX Quantum* **6**, 040325 (Nov 2025). <https://doi.org/10.1103/1gjs-2rhx>, <https://link.aps.org/doi/10.1103/1gjs-2rhx>
48. Kissinger, A.: Phase-free ZX diagrams are CSS codes (...or how to graphically grok the surface code) (Apr 2022), <http://arxiv.org/abs/2204.14038>
49. Kissinger, A., van de Wetering, J.: Picturing Quantum Software: An Introduction to the ZX-Calculus and Quantum Compilation. Preprint (2024), <https://github.com/zxcalc/book/>
50. Kubica, A., Yoshida, B., Pastawski, F.: Unfolding the color code. *New Journal of Physics* **17**(8), 083026 (2015)
51. Li, C., Preskill, J., Xu, Q.: Transversal dimension jump for product qldpc codes (2025), <https://arxiv.org/abs/2510.07269>
52. Li, S.M., Mosca, M., Ross, N.J., van de Wetering, J., Zhao, Y.: A complete and natural rule set for multi-qudit clifford circuits. *Electronic Proceedings in Theoretical Computer Science* **426**, 23–78 (Aug 2025). <https://doi.org/10.4204/eptcs.426.2>, <http://dx.doi.org/10.4204/EPTCS.426.2>

53. Lysaght, L., Goubault, T., Sinnott, P., Mansfield, S., Emeriau, P.E.: Quantum circuit compression using qubit logic on qudits (2024), <https://arxiv.org/abs/2411.03878>
54. Mato, K., Hillmich, S., Wille, R.: Compression of qubit circuits: Mapping to mixed-dimensional quantum systems. In: 2023 IEEE International Conference on Quantum Software (QSW). pp. 155–161 (2023). <https://doi.org/10.1109/QSW59989.2023.00027>
55. Mato, K., Ringbauer, M., Burgholzer, L., Wille, R.: Mqt qudits: A software framework for mixed-dimensional quantum computing (2024), <https://arxiv.org/abs/2410.02854>
56. Meth, M., Zhang, J., Haase, J.F., Edmunds, C., Postler, L., Jena, A.J., Steiner, A., Dellantonio, L., Blatt, R., Zoller, P., Monz, T., Schindler, P., Muschik, C., Ringbauer, M.: Simulating two-dimensional lattice gauge theories on a qudit quantum computer. *Nature Physics* **21**(4), 570–576 (Apr 2025). <https://doi.org/10.1038/s41567-025-02797-w>, <https://doi.org/10.1038/s41567-025-02797-w>
57. Miao, K.C., McEwen, M., Atalaya, J., Kafri, D., Pryadko, L.P., Bengtsson, A., Opremcak, A., Satzinger, K.J., Chen, Z., Klimov, P.V., Quintana, C., Acharya, R., Anderson, K., Ansmann, M., Arute, F., Arya, K., Asfaw, A., Bardin, J.C., Bourassa, A., Bovaird, J., Brill, L., Buckley, B.B., Buell, D.A., Burger, T., Burkett, B., Bushnell, N., Campero, J., Chiaro, B., Collins, R., Conner, P., Crook, A.L., Curtin, B., Debroy, D.M., Demura, S., Dunsworth, A., Erickson, C., Fatemi, R., Ferreira, V.S., Burgos, L.F., Forati, E., Fowler, A.G., Foxen, B., Garcia, G., Gidney, W., Gidney, C., Giustina, M., Gosula, R., Dau, A.G., Gross, J.A., Hamilton, M.C., Harrington, S.D., Heu, P., Hilton, J., Hoffmann, M.R., Hong, S., Huang, T., Huff, A., Iveland, J., Jeffrey, E., Jiang, Z., Jones, C., Kelly, J., Kim, S., Kostritsa, F., Kreikebaum, J.M., Landhuis, D., Laptev, P., Laws, L., Lee, K., Lester, B.J., Lill, A.T., Liu, W., Locharla, A., Lucero, E., Martin, S., Megrant, A., Mi, X., Montazeri, S., Morvan, A., Naaman, O., Neeley, M., Neill, C., Nersisyan, A., Newman, M., Ng, J.H., Nguyen, A., Nguyen, M., Potter, R., Rocque, C., Roushan, P., Sankaragomathi, K., Schurkus, H.F., Schuster, C., Shearn, M.J., Shorter, A., Shutty, N., Shvarts, V., Skrzynny, J., Smith, W.C., Sterling, G., Szalay, M., Thor, D., Torres, A., White, T., Woo, B.W.K., Yao, Z.J., Yeh, P., Yoo, J., Young, G., Zalcman, A., Zhu, N., Zobrist, N., Neven, H., Smelyanskiy, V., Petukhov, A., Korotkov, A.N., Sank, D., Chen, Y.: Overcoming leakage in quantum error correction. *Nature Physics* **19**(12), 1780–1786 (Dec 2023). <https://doi.org/10.1038/s41567-023-02226-w>, <https://www.nature.com/articles/s41567-023-02226-w>
58. Nakanishi, K.M., Todo, S.: Systematic construction of multi-controlled pauli gate decompositions with optimal t -count (2024), <https://arxiv.org/abs/2410.00910>
59. Petit, L., Russ, M., Eenink, G.H., Lawrie, W.I., Clarke, J.S., Vandersypen, L.M., Veldhorst, M.: Design and integration of single-qubit rotations and two-qubit gates in silicon above one kelvin (2022)
60. Pino, J.M., Dreiling, J.M., Figgatt, C., Gaebler, J.P., Moses, S.A., Allman, M.S., Baldwin, C.H., Foss-Feig, M., Hayes, D., Mayer, K., Ryan-Anderson, C., Neyenhuis, B.: Demonstration of the trapped-ion quantum CCD computer architecture. *Nature* **592**(7853), 209–213 (apr 2021). <https://doi.org/10.1038/s41586-021-03318-4>
61. Poór, B., Booth, R.I., Carette, T., van de Wetering, J., Yeh, L.: The qupit stabiliser zx-travaganza: Simplified axioms, normal forms and graph-theoretic simplification. *Electronic Proceedings in Theoretical Computer Science* **384**, 220–264

- (Aug 2023). <https://doi.org/10.4204/eptcs.384.13>, <http://dx.doi.org/10.4204/EPTCS.384.13>
62. Prakash, S.: Magic state distillation with the ternary golay code. *Proceedings of the Royal Society A: Mathematical, Physical and Engineering Sciences* **476**(2241), 20200187 (2020). <https://doi.org/10.1098/rspa.2020.0187>, <https://royalsocietypublishing.org/doi/abs/10.1098/rspa.2020.0187>
 63. Prakash, S., Jain, A., Kapur, B., Seth, S.: Normal form for single-qutrit clifford+ t operators and synthesis of single-qutrit gates. *Physical Review A* **98**(3) (Sep 2018). <https://doi.org/10.1103/physreva.98.032304>, <http://dx.doi.org/10.1103/PhysRevA.98.032304>
 64. Ranchin, A.: Depicting qudit quantum mechanics and mutually unbiased qudit theories. *Electronic Proceedings in Theoretical Computer Science* **172**, 68–91 (dec 2014). <https://doi.org/10.4204/eptcs.172.6>
 65. Ringbauer, M., Meth, M., Postler, L., Stricker, R., Blatt, R., Schindler, P., Monz, T.: A universal qudit quantum processor with trapped ions. *Nature Physics* **18**(9), 1053–1057 (Sep 2022). <https://doi.org/10.1038/s41567-022-01658-0>, <https://www.nature.com/articles/s41567-022-01658-0>
 66. Roy, P., van de Wetering, J., Yeh, L.: The qudit zh-calculus: Generalised toffoli+hadamard and universality. *Electronic Proceedings in Theoretical Computer Science* **384**, 142–170 (Aug 2023). <https://doi.org/10.4204/eptcs.384.9>, <http://dx.doi.org/10.4204/EPTCS.384.9>
 67. Selinger, P.: Quantum circuits of t -depth one. *Physical Review A* **87**(4), 042302 (Apr 2013). <https://doi.org/10.1103/PhysRevA.87.042302>
 68. Sheldon, S., Magesan, E., Chow, J.M., Gambetta, J.M.: Procedure for systematically tuning up cross-talk in the cross-resonance gate. *Phys. Rev. A* **93**, 060302 (Jun 2016). <https://doi.org/10.1103/PhysRevA.93.060302>
 69. Shende, V.V., Markov, I.L.: On the cnot-cost of toffoli gates. *Quantum Info. Comput.* **9**(5), 461–486 (May 2009)
 70. de Silva, N.: Efficient quantum gate teleportation in higher dimensions. *Proceedings of the Royal Society A: Mathematical, Physical and Engineering Sciences* **477**(2251) (Jul 2021). <https://doi.org/10.1098/rspa.2020.0865>, <http://dx.doi.org/10.1098/rspa.2020.0865>
 71. Srivastav, V., Valencia, N.H., McCutcheon, W., Leedumrongwatthanakun, S., Designolle, S., Uola, R., Brunner, N., Malik, M.: Quick quantum steering: Overcoming loss and noise with qudits. *Physical Review X* **12**(4) (Nov 2022). <https://doi.org/10.1103/physrevx.12.041023>, <http://dx.doi.org/10.1103/PhysRevX.12.041023>
 72. Steane, A.M.: Active stabilization, quantum computation, and quantum state synthesis. *Phys. Rev. Lett.* **78**, 2252–2255 (Mar 1997). <https://doi.org/10.1103/PhysRevLett.78.2252>, <https://link.aps.org/doi/10.1103/PhysRevLett.78.2252>
 73. Steane, A.M.: Active stabilization, quantum computation, and quantum state synthesis. *Physical Review Letters* **78**(11), 2252–2255 (Mar 1997). <https://doi.org/10.1103/physrevlett.78.2252>, <http://dx.doi.org/10.1103/PhysRevLett.78.2252>
 74. Townsend-Teague, A., Meichanetzidis, K.: Simplification Strategies for the Qutrit ZX-Calculus (Jun 2022). <https://doi.org/10.48550/arXiv.2103.06914>
 75. Wang, Q.: Qutrit ZX-calculus is Complete for Stabilizer Quantum Mechanics (Mar 2018). <https://doi.org/10.48550/arXiv.1803.00696>, <http://arxiv.org/abs/1803.00696>, arXiv:1803.00696

76. Wang, Q., Bian, X.: Qutrit dichromatic calculus and its universality. *Electronic Proceedings in Theoretical Computer Science* **172**, 92–101 (Dec 2014). <https://doi.org/10.4204/eptcs.172.7>, <http://dx.doi.org/10.4204/EPTCS.172.7>
77. Weggemans, J.R., Urech, A., Rausch, A., Spreeuw, R., Boucherie, R., Schreck, F., Schoutens, K., Minář, J., Speelman, F.: Solving correlation clustering with QAOA and a rydberg qudit system: a full-stack approach. *Quantum* **6**, 687 (apr 2022). <https://doi.org/10.22331/q-2022-04-13-687>, <https://doi.org/10.22331/q-2022-04-13-687>
78. van de Wetering, J.: Constructing quantum circuits with global gates. *New Journal of Physics* **23**(4), 043015 (apr 2021). <https://doi.org/10.1088/1367-2630/abf1b3>
79. Wetering, J.v.d., Yeh, L.: Building Qutrit Diagonal Gates from Phase Gadgets (Nov 2023). <https://doi.org/10.48550/arXiv.2204.13681>
80. Yeh, L.: Transdimensional quantum computation: the graphical novel. Ph.D. thesis, University of Oxford (2026)
81. Yeh, L., Huang, J., Kissinger, A., Li, S.M., van de Wetering, J.: A three-way normal form for stabiliser codes across zx diagrams, circuits, and tableaux (2026), in preparation
82. Yeh, L., van de Wetering, J.: Constructing All Qutrit Controlled Clifford+T gates in Clifford+T, p. 28–50. Springer International Publishing (2022). https://doi.org/10.1007/978-3-031-09005-9_3, http://dx.doi.org/10.1007/978-3-031-09005-9_3
83. Yu, N., Duan, R., Ying, M.: Five two-qubit gates are necessary for implementing the toffoli gate. *Phys. Rev. A* **88**, 010304 (Jul 2013). <https://doi.org/10.1103/PhysRevA.88.010304>, <https://link.aps.org/doi/10.1103/PhysRevA.88.010304>
84. Zi, W., Li, Q., Sun, X.: Optimal synthesis of multi-controlled qudit gates. In: 2023 60th ACM/IEEE Design Automation Conference (DAC). pp. 1–6 (2023). <https://doi.org/10.1109/DAC56929.2023.10247925>

A Qutrit ZX-calculus Rules

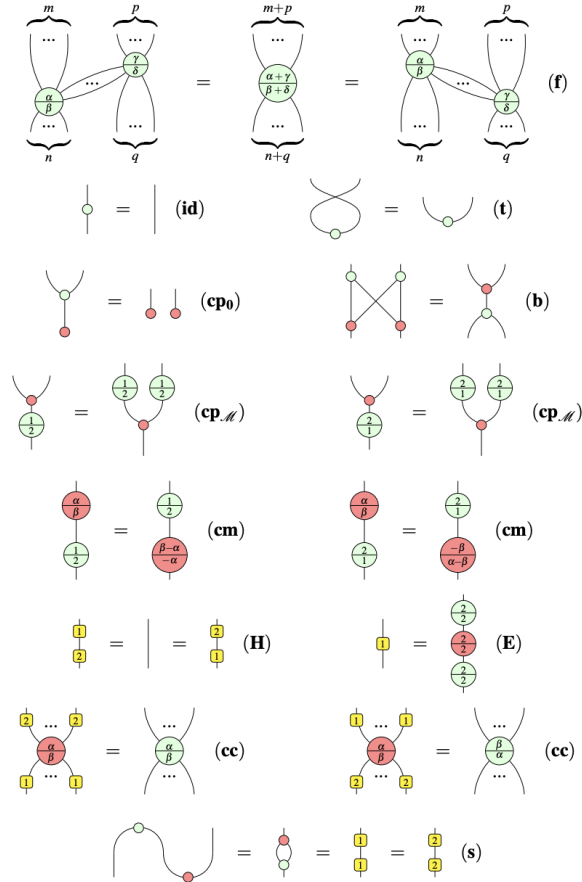


Fig. 1: Rewrite rules for the qutrit ZX-calculus, reprinted from Figure 1 in [74]

A.1 Pushing through the encoder

“Pushing through the encoder” refers to the idea that, for any encoder E for a CSS code (which is a phase-free diagram that is an isometry), any diagram \mathcal{D} on the left of E (which is the logical operator) has a corresponding diagram \mathcal{D}_P on the right of E (which is a physical implementation of \mathcal{D}). This was developed for qubit CSS codes in [42]. We generalize this idea to qutrits as follows:

Lemma 2 (“Pushing through the encoder” (PTE) for qutrits). *Let E be the encoder of a qutrit CSS code. For any ZX diagram \mathcal{D}_L on the left of E , it has a corresponding diagram \mathcal{D}_P on the right of E such that $E\mathcal{D}_L = \mathcal{D}_P E$.*

Proof. Similar to the proof for Proposition 3.1 of [42], any Z or X spiders in \mathcal{D}_L on the logical wires that has phases or multiple legs can be unfused so that each logical Z or X spider on the logical qutrit wire has just one external wire. Using strong complementarity with the corresponding choice of diagram of the encoder (for a Z spider, use X-Z normal form, and for X spider, use Z-normal form), one can “push” this supporting leg of the diagram to the right side. For any diagram \mathcal{D} supported on an arbitrary number of logical wires,

(26)

Note that for qutrits, there may be double wires (which can be represented as a single wire with a “D” dualizer box) in encoders connecting Z and X spiders. The connectivity degree (single or double wires) for each supporting logical qubit to \mathcal{D} is preserved for the corresponding X spider for that logical on the right. \square

B Deconstruction of the Qubit $[[8, 3, 2]]$ Code

B.1 Circuit Synthesis and ZX-calculus View

Here, we will demonstrate the well-known example of the transversal CCZ gate of the $[[8, 3, 2]]$ code [11] (also called the smallest interesting color code, an instance of transversal CCZ gates described in [50]), in the ZX-calculus.

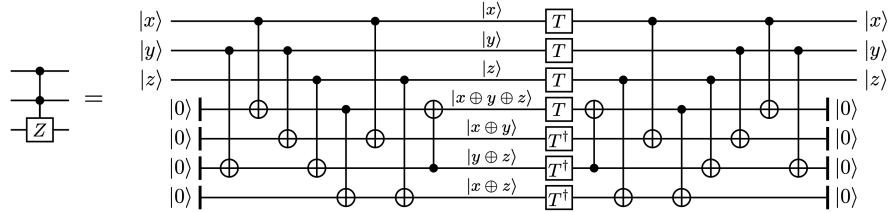
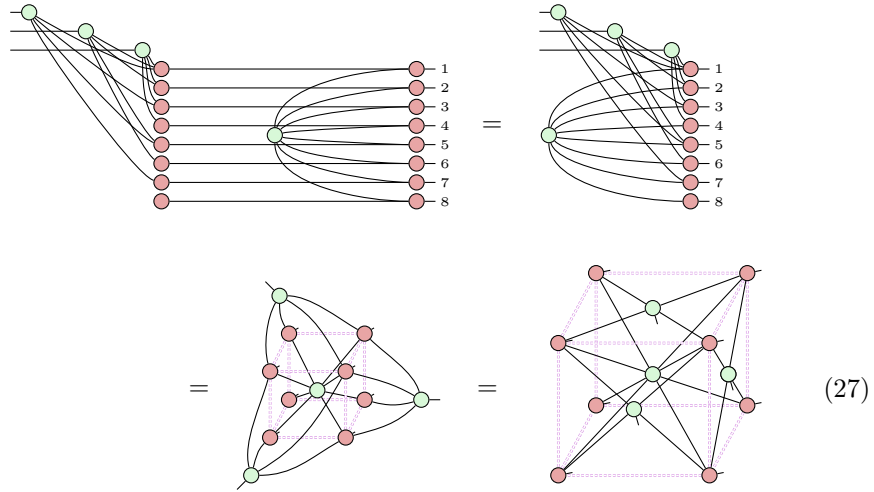


Fig. 2: Figure for a T-depth one decomposition of the qubit CCZ gate, reprinted from [67, Figure 1].

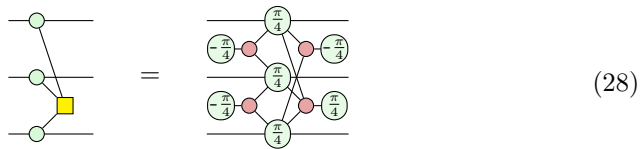
In an observation credited to Campbell [11], the above circuit consists of a CNOT circuit unitary embedding E , a layer of T and T^\dagger gates, and E^\dagger . This

therefore defines a $[[7, 3, 1]]$ code. Being distance 1, it has no error-correcting capabilities. To improve the code distance, it suffices to add to the encoder E (whose ZX diagram first appeared in [24]) one physical qubit, and a weight 8 X-type stabilizer generator connected to all 8 physical qubits:



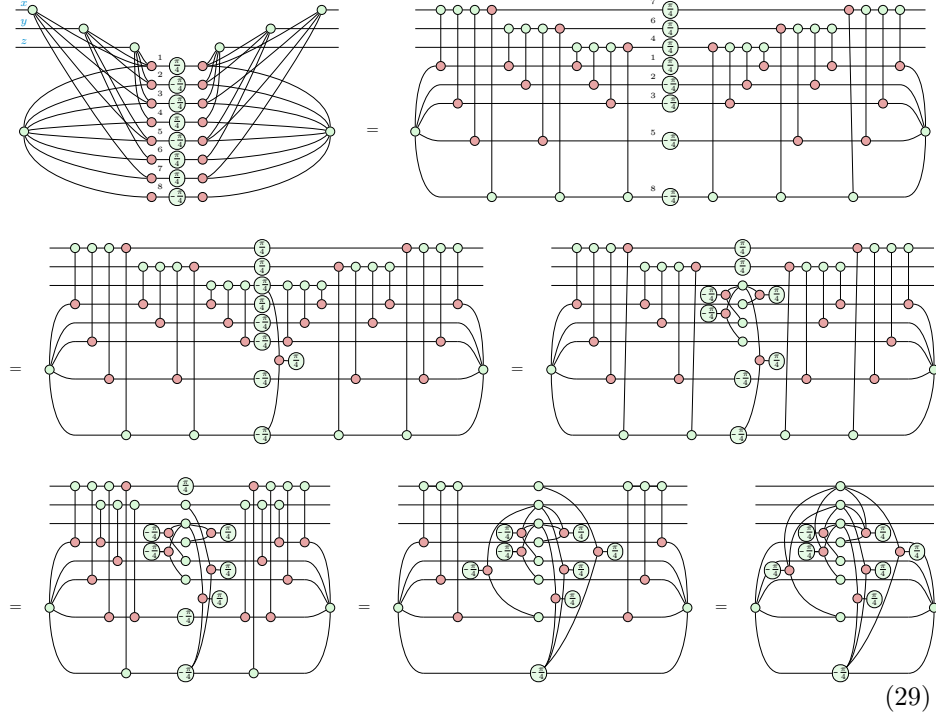
B.2 Verifying Transversal CCZ Preservation

This construction preserves the transversal CCZ gate, resulting in the $[[8, 3, 2]]$ code. To show this, we will use the following fact about the phase polynomial representation of the CCZ gate as the map that acts as $|x, y, z\rangle \mapsto (-1)^{x \cdot y \cdot z} |x, y, z\rangle$, where x, y, z are bits denoting computational basis states. As was shown for qutrits in [79], the qubit CCZ gate is identified by the exponent of (-1) being a multiplicative expression $x \cdot y \cdot z$; this can be replaced by an equivalent expression summing over modular addition. For this reason, the qubit CCZ gate is equal to the following spider nest of phase gadgets:

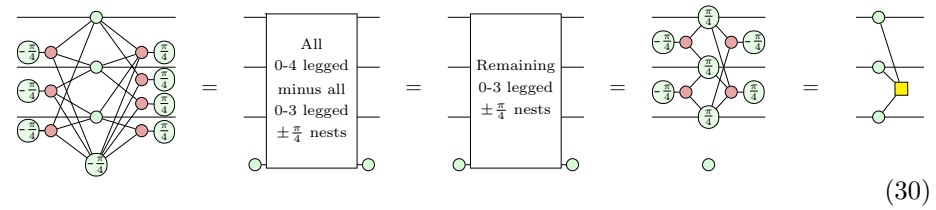


If instead all phases here are $\pm \frac{\pi}{2}$, then instead of the CCZ gate, this is the identity map on three qubits. More generally, for n qubits, having one of all possible connectivity phase gadgets of 0 - n legs, of phases $\pm \frac{\pi}{2^{n-2}}$ where the sign matches the parity of the number of legs, is equal to the n -qubit identity map.

We can substitute the encoder E of the $[[8, 3, 2]]$ code from [24], to verify that $L = E; P; E^\dagger$ where L is the CCZ gate, and $P = TT^\dagger T^\dagger TT^\dagger TTT^\dagger$.



Continuing from the last step, we now utilize the above observation to recognize that what we have is the spider nest of all 0-4 legged $\mp \frac{\pi}{4}$ phase gadgets, conjugated by all 0-3 legged $\pm \frac{\pi}{4}$ phase gadgets on the upper three qubits. Therefore, we can then apply all 0-4 legged $\mp \frac{\pi}{4}$ phase gadgets, which equals the identity. The end result is precisely the CCZ gate.



C Proofs for Magic State Distillation and Injection

C.1 CCZ Magic State Distillation

Here, we give a graphical portrayal of magic state distillation. We have just derived that the logical CCZ gate in the $[[8, 3, 2]]$ code is physically implemented

by 8 T and T^\dagger gates:

$$(31)$$

Taking the conjugate transpose of the above equation and inputting $|+\rangle^{\otimes 8}$, the ideal decoder acts on 8 T and T^\dagger magic states as:

$$(32)$$

Substituting in the Z-X GPF of the encoder, the $|+\rangle$ states copy and fuse, leaving just the three-legged H-box.

$$(33)$$

In other words, the decoding of 8 T and T^\dagger magic states results in a less noisy CCZ magic state.

Were it distilling the $|0\rangle$ -controlled Z magic state from the inner CSS code of our qutrit $[[6, 2, 2]]$ code, the proof steps are identical to the above. Indeed, this proof applies for distilling magic states of any transversal diagonal gate in a CSS code whose X and Z logical operators are realized by physical X's and Z's respectively, i.e. whose encoder is a phase-free isometry in the ZX-calculus.

C.2 CCZ Magic State Injection for Prime-Dimensional Qudits

Proposition 2. *As is the case for qubits, for any odd prime qudit dimension, the Toffoli and CCZ gates are in the third level of the Clifford hierarchy.*

Proof. Noting the ZX diagram interpretations of the Z-basis states:

$$\begin{array}{c} \frac{2a}{a} \\ \circlearrowleft \\ \hline \end{array} = |a\rangle \quad \begin{array}{c} \frac{a}{2a} \\ \circlearrowleft \\ \hline \end{array} = \langle a| \quad \begin{array}{c} \frac{2a}{a} \\ \circlearrowright \\ \hline \end{array} = X^a \quad (34)$$

Pauli Z directly commutes through the CCZ gate because both are diagonal in the Z basis. We can commute Pauli X through the CCZ gate as follows:

$$\begin{array}{c} X^{-j} \\ \hline \end{array} \text{CCZ} = \begin{array}{c} \frac{a}{2j} \\ \circlearrowleft \\ \hline \end{array} \begin{array}{c} \text{---} \\ \text{---} \\ \text{---} \end{array} = \begin{array}{c} \frac{a}{2j} \\ \circlearrowleft \\ \hline \end{array} \begin{array}{c} \text{---} \\ \text{---} \\ \text{---} \end{array} \begin{array}{c} \frac{a}{2j} \\ \circlearrowleft \\ \hline \end{array} = \begin{array}{c} \text{CCZ} \\ \hline \end{array} \begin{array}{c} X^{-j} \\ \hline \end{array} \begin{array}{c} \text{---} \\ \text{---} \\ \text{---} \end{array} \begin{array}{c} \text{CZ}^j \\ \hline \end{array} \quad (35)$$

□

As it is in the third level of the Clifford hierarchy, the Toffoli and CCZ gates admit magic state injection for any prime qudit dimension. Moreover, both these gates are semi-Clifford [70]:

Definition 9. A gate G is semi-Clifford if it admits a decomposition $G = C_2 D C_1$, as a diagonal gate in some level of the Clifford hierarchy D , pre- and post-composed by Clifford gates C_1 and C_2 respectively.

Therefore, a more efficient (halving the number of ancillae qudits) gate teleportation can be utilized [70]:

Proposition 3. For any prime qudit dimension, the CCZ gate is deterministically implementable by one round of the below magic state injection protocol, with one copy of the CCZ magic state.

Proof. The multiqutrit case of the teleportation circuit follows from parallelism of the singlequtrit case.

$$\begin{array}{c} \text{---} \\ \text{---} \end{array} \begin{array}{c} \frac{a}{2a} \\ \circlearrowleft \\ \hline \end{array} = \begin{array}{c} \text{---} \\ \text{---} \end{array} \begin{array}{c} \frac{a}{2a} \\ \circlearrowleft \\ \hline \end{array} = \begin{array}{c} \text{---} \\ \text{---} \end{array} \begin{array}{c} \frac{a}{2a} \\ \circlearrowleft \\ \hline \end{array} \begin{array}{c} \frac{a}{2a} \\ \circlearrowleft \\ \hline \end{array} = \begin{array}{c} \text{---} \\ \text{---} \end{array} \begin{array}{c} \frac{a}{2a} \\ \circlearrowleft \\ \hline \end{array} = \begin{array}{c} \text{---} \\ \text{---} \end{array} \begin{array}{c} \frac{a}{2a} \\ \circlearrowleft \\ \hline \end{array} = \begin{array}{c} \text{---} \\ \text{---} \end{array} \quad (36)$$

By commuting the intended gate to teleport (the CCZ gate) through the three-qubit teleportation circuit, we get that the CCZ magic state can be teleported by that circuit, with Pauli X and Clifford CZ gate corrections controlled on the measurement outcomes.

$$\begin{array}{c} \text{---} \\ \text{---} \\ \text{---} \\ \text{---} \end{array} \begin{array}{c} \frac{a}{2a} \\ \circlearrowleft \\ \hline \end{array} \begin{array}{c} \frac{a}{2a} \\ \circlearrowleft \\ \hline \end{array} \begin{array}{c} \frac{b}{2b} \\ \circlearrowleft \\ \hline \end{array} \begin{array}{c} \frac{b}{2b} \\ \circlearrowleft \\ \hline \end{array} \begin{array}{c} \frac{c}{2c} \\ \circlearrowleft \\ \hline \end{array} \begin{array}{c} \frac{c}{2c} \\ \circlearrowleft \\ \hline \end{array} = \begin{array}{c} \text{---} \\ \text{---} \\ \text{---} \\ \text{---} \end{array} \begin{array}{c} \frac{a}{2a} \\ \circlearrowleft \\ \hline \end{array} \begin{array}{c} \frac{a}{2a} \\ \circlearrowleft \\ \hline \end{array} \begin{array}{c} \frac{b}{2b} \\ \circlearrowleft \\ \hline \end{array} \begin{array}{c} \frac{b}{2b} \\ \circlearrowleft \\ \hline \end{array} \begin{array}{c} \frac{c}{2c} \\ \circlearrowleft \\ \hline \end{array} \begin{array}{c} \frac{c}{2c} \\ \circlearrowleft \\ \hline \end{array} \quad (37)$$

□

C.3 $|0\rangle$ -Controlled Z Injection

We start by deriving the ZX diagram for the $|0\rangle$ -controlled Z gate, by conjugating the $|0\rangle$ -controlled X^\dagger from [66, Equation 5]:

$$\begin{array}{c} \textcircled{0} \\ | \\ \square{Z} \end{array} = \begin{array}{c} \textcircled{0} \\ | \\ \square{H} \square{X^\dagger} \square{H^\dagger} \end{array} = \begin{array}{c} \textcircled{1} \\ | \\ \textcircled{2} \textcircled{1} \textcircled{2} \textcircled{1} \end{array} = \begin{array}{c} \textcircled{1} \\ | \\ \textcircled{2/i} \end{array} \quad (38)$$

Its magic state is obtained by inputting $|++\rangle$:

$$|ZCZ\rangle = \begin{array}{c} \textcircled{1} \\ | \\ \textcircled{2/i} \end{array} = \begin{array}{c} \textcircled{1} \\ | \\ \textcircled{2/i} \end{array} \quad (39)$$

The standard injection circuit is below. When the measurement outcome is $\langle 00|$, i.e. both a and b are zero, then we have that this circuit implements the $|0\rangle$ -controlled Z gate.

$$\begin{array}{c} \textcircled{0} \\ | \\ \square{H^2} \square{X} \textcircled{a} \\ | \\ \square{H^2} \square{X} \textcircled{b} \end{array} = \begin{array}{c} \textcircled{1} \\ | \\ \textcircled{2a/a} \textcircled{1} \textcircled{2} \textcircled{1} \end{array} = \begin{array}{c} \textcircled{1} \\ | \\ \textcircled{2a/a} \textcircled{1} \textcircled{2} \textcircled{1} \end{array} = \begin{array}{c} \textcircled{1} \\ | \\ \textcircled{2a/a} \textcircled{1} \textcircled{2} \textcircled{1} \end{array} \quad (40)$$

To see if this can be deterministically injectable, we will need the following lemma:

Lemma 3. For $a, b \in \mathbb{Z}$,

$$\begin{array}{c} \textcircled{a/2a} \textcircled{b} \end{array} = \left\{ \begin{array}{l} \textcircled{a/2a} \textcircled{0} \textcircled{0} = \textcircled{0} \textcircled{0/0}, b=0 \\ \textcircled{1} \textcircled{2a/a} \textcircled{2} \textcircled{1} = \textcircled{1} \textcircled{2a/a} \textcircled{b}, b=1 \\ \textcircled{2} \textcircled{a/2a} \textcircled{1} \textcircled{2} = \textcircled{2} \textcircled{a/2a} \textcircled{b}, b=2 \end{array} \right\} = \textcircled{b} \textcircled{2ab/ab} \quad (41)$$

We can thereafter push both X corrections from measurement through the magic state, to obtain a diagonal Clifford correction.

(42)

Pauli Z commutes with the $|0\rangle$ -controlled gate because they're both gates diagonal in the Z-basis. Therefore, this proves that the $|0\rangle$ -controlled gate is in the third level of the Clifford hierarchy, because pushing through any Pauli operator results in a correction that is Clifford, i.e. in the second level of the Clifford hierarchy.

We can then append to our earlier circuit the inverse of this error term, as a correction parametrized by the measurement outcome.

(43)

As a result, irrespective of measurement outcome, we have deterministic implementation of the $|0\rangle$ -controlled gate by magic state injection.

C.4 Implementing the AND Gate via Magic State Distillation and Injection

Up to now, we have been working with the simpler setting—injecting diagonal logical gates distilled in a CSS code whose logical X’s and Z’s are implemented by physical X’s and Z’s respectively. Our goal is now to distill and inject the AND gate into any qutrit CSS code, so long as you have the capability to do fault-tolerant S gates (for instance, transversal in the code or via subsequent injection). Essentially, we want the protocol to not require the code to have a transversal H gate, i.e. be self-dual.

In the two-qutrit unitary U that fixes our logical operators such that the transversal operation is AND instead of $|0\rangle$ -controlled Z, it is the CX gate that causes a problem with injecting the AND magic state directly such that it cannot be corrected as to be deterministic. Instead, as done for U^\dagger below, we push the CX out to be the outermost gate, in order to inject the remaining gates as part of the magic state. As we are injecting into a CSS code, the CX can be executed transversally conjugating the injection.

$$\text{Diagram 1} = \text{Diagram 2} = \text{Diagram 3} \quad (44)$$

By decoding 3 T and 3 T^\dagger states (which can be recursively distilled) in the code without this CX, we get a magic state for the AND gate up to this CX.

$$\text{Diagram 1} = \text{Diagram 2} = \text{Diagram 3} = \text{Diagram 4} = \text{Diagram 5} = \text{Diagram 6} = \text{Diagram 7} \quad (45)$$

We can then perform deterministic injection, through proving this as a modification of our earlier protocol in Equation (43).

(46)

The resulting correction is a Clifford unitary where all but one gate—the $Z(2b, 2b)$ gate—are Pauli or CX gates, and hence transversally implementable on CSS codes [35]. As a single-qutrit diagonal Clifford unitary, the $Z(2b, 2b)$ gate can be implemented by the standard magic state injection protocol.

The remaining piece of the puzzle, is that the protocol measures two qutrits in two different bases, X and Z. Presume we have access to the $|0+\rangle$ logical state in the code as a resource. If there are more than two logical qubits per code block, the resource state should be $|0+ \dots +\rangle$ or $|0\dots 0+\rangle$, depending on whether you want to measure one logical qubit in the Z or X basis respectively.

Say that we want to measure logical $\overline{\langle a | \otimes I}$, where I is the identity operation on all logical qutrits except the one we want to measure; without loss of generality, let us say we want to measure the first logical qutrit. Observe that the $|0+\rangle = E|0+\rangle$ state is representable as a phase-free ZX diagram, where the logical qutrit you want to measure is set to $|0\rangle$ and the rest to $|+\rangle$.

(47)

The resulting ZX diagram is a bipartite graph whose connectivity is that of logical Z_1 and Z stabilizer generators of the code. This correspondence between ZX diagrams of stabilizer codes, stabilizer tableaux, and Tanner graphs is detailed in [81].

Injecting this resource state yields the desired Z-basis measurement of the first logical qutrit.

$$(48)$$

It additionally performs Steane-style syndrome measurement [73] of the Z checks.

Exchanging the roles of Z and X, and $|0\rangle$ and $|+\rangle$, likewise enables measuring $I \otimes \langle b| H$ in addition to Steane-style syndrome measurement of the X checks.

D Gate Counts for Qutrit Emulation of Qubit and Binary Operations

D.1 Emulating the qubit X, Z, S, CX and CZ gates

The qubit Hadamard and CNOT operations cannot be emulated utilizing qutrit Clifford gates [7]. Moreover, we can show that the qubit Hadamard gate cannot be exactly and deterministically emulated using qutrit Clifford+T, despite this being an approximately universal gate set. This follows from normal forms for single-qutrit Clifford+T operators, which impose the necessary but not sufficient condition that the matrix entries belong to the ring $\mathbb{Z} \left[\frac{1}{1-\zeta} \right]$, as independently determined by Prakash, Jain, Kapur, and Seth [63]; and Glaudell, Ross, and Taylor [29]:

Definition 10 ($\mathbb{Z} \left[\frac{1}{1-\zeta} \right]$). Let $\zeta = e^{i\frac{2\pi}{9}}$. The matrix elements of all single-qutrit Clifford+T unitaries must be elements of the ring

$$\mathbb{Z} \left[\frac{1}{1-\zeta} \right] = \left\{ \frac{A}{(1-\zeta)^k} \mid A \in \mathbb{Z}[\zeta], k \in \mathbb{N} \right\} \quad (49)$$

where

$$\mathbb{Z}[\zeta] = \left\{ \sum_{i=0}^5 a_i(\zeta)^i \mid \forall i, a_i \in \mathbb{Z} \right\} \quad (50)$$

Because $\frac{1}{\sqrt{2}}$ is not in the ring in Definition 10, it is impossible to exactly and deterministically emulate the qubit Hadamard gate utilizing single-qutrit Clifford+T gates. In general, the qubit Clifford operations do not neatly embed in the qutrit Clifford fragment.

In spite of this, we can still emulate quite a few qubit gates using qutrits. The qubit X gate can be emulated by the qutrit Clifford X_{01} gate. The qubit Z gate can be emulated by Clifford equivalence to the qutrit R gate:

$$\text{qubit } Z \stackrel{e}{\leftarrow} X_{12} R X_{12} \quad (51)$$

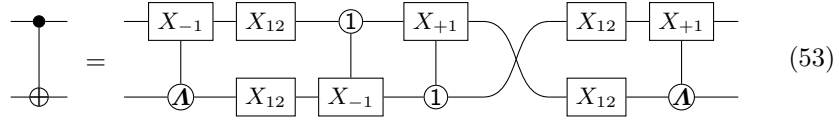
Likewise, the qubit S gate can be emulated by Clifford equivalence to the qutrit \sqrt{R} gate:

$$\text{qubit } S \stackrel{e}{\leftarrow} X_{12} \sqrt{R} X_{12} \quad (52)$$

Extending magic state injection of the R gate [2], despite being nowhere in the Clifford hierarchy, it can be shown that the $\sqrt{R} = \text{diag}(1, 1, i)$ gate admits implementation by a repeat-until-success injection protocol of the $(1, 1, i)^\top$ state, where the probability of success rapidly converges to 1 with the number of rounds.

Lemma 4 ([7]). *The qubit CX gate can be emulated by qutrit Clifford+T gates unitarily without ancillae, with T-count 6 and Clifford CX-count 8.*

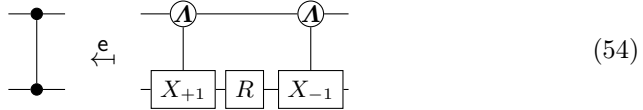
Proof. For reference, the decomposition by Bocharov, Roetteler, and Svore [7, Proposition 4] is given as a circuit diagram below:



Like the qubit SWAP gate, the qutrit SWAP gate can be decomposed as three of the same two-qutrit gate applied successively in alternating directions. By optimizing thereafter, the Clifford CX-count can be further reduced to 8. \square

Lemma 5. *Utilizing one R gate, we can exactly emulate the qubit CZ gate.*

Proof.



On qubit input states $|00\rangle$, $|01\rangle$, and $|10\rangle$, the states' sum modulo 3 is 0 or 1, and so no phase factor is applied. When the input state is $|11\rangle$, the states' sum modulo 3 is 2, and so a phase factor of -1 is applied. \square

This improves on the three R-count decomposition achieved by conjugating the control of the $|2\rangle$ -controlled qubit Z gate from [79] by X_{12} .

A qubit Toffoli gate can be built from qutrit gates using the decomposition by Gokhale et. al. [5, 32]:

$$\begin{array}{c}
 |q_0\rangle \text{---} \bullet \text{---} \\
 |q_1\rangle \text{---} \bullet \text{---} \\
 |q_2\rangle \text{---} \oplus \text{---}
 \end{array}
 \xrightarrow{e}
 \begin{array}{c}
 |q_0\rangle \text{---} \textcircled{1} \text{---} \\
 |q_1\rangle \text{---} \boxed{X_{+1}} \text{---} \textcircled{2} \text{---} \boxed{X_{-1}} \text{---} \\
 |q_2\rangle \text{---} \boxed{X_{01}} \text{---}
 \end{array}
 \quad (56)$$

To exactly emulate the qubit CCX gate, the X gate on the target qutrit must be X_{01} . In their presentation of this gate they simply denoted the gate on the target qutrit as X , referring to any of the five single-qutrit computational basis permutation gates. The action of the gate is irrelevant for the cases where any of the input qutrits are in the $|2\rangle$ state, making it more efficient to use Clifford CX gates to replace the top two controlled gates:

$$\begin{array}{c}
 |q_0\rangle \text{---} \textcircled{1} \text{---} \textcircled{2} \text{---} \\
 |q_1\rangle \text{---} \boxed{X_{+1}} \text{---} \boxed{X_{-1}} \text{---}
 \end{array}
 =
 \begin{array}{c}
 \text{---} \textcircled{A} \text{---} \\
 \text{---} \boxed{X_{+1}} \text{---}
 \end{array}
 \quad (57)$$

$$\begin{array}{c}
 |q_0\rangle \text{---} \textcircled{1} \text{---} \textcircled{2} \text{---} \\
 |q_1\rangle \text{---} \boxed{X_{-1}} \text{---} \boxed{X_{+1}} \text{---}
 \end{array}
 =
 \begin{array}{c}
 \text{---} \textcircled{A} \text{---} \\
 \text{---} \boxed{X_{-1}} \text{---}
 \end{array}
 \quad (58)$$

Without compromising the correctness of the qubit Toffoli gate, the above decomposition in Equation (56) was modified by Bocharov, Roetteler, and Svore as follows [7, Proposition 6]:

$$\begin{array}{c}
 |q_0\rangle \text{---} \bullet \text{---} \\
 |q_1\rangle \text{---} \bullet \text{---} \\
 |q_2\rangle \text{---} \boxed{X} \text{---}
 \end{array}
 \xrightarrow{e}
 \begin{array}{c}
 \text{---} \textcircled{A} \text{---} \\
 \text{---} \textcircled{A} \text{---} \\
 \text{---} \textcircled{2} \text{---} \\
 \text{---} \boxed{X} \text{---}
 \end{array}
 \quad (59)$$

They concluded that the qubit CCX gate takes 15 T-gates to emulate with qutrit Clifford+T gates, taking the bottom gate to be the $|2\rangle$ -controlled X_{01} gate, as the X_{01} gate emulates the qubit X gate. They lower the T-count to 12 by adding one clean ancilla.

We show that the T-count can be 12 without ancillae, by $|2\rangle$ -controlling an emulation of the qubit X gate instead of the X_{01} gate.

Proposition 4. *The $|2\rangle$ -controlled qubit X gate, which executes the qubit X gate if and only if the control qutrit is in the $|2\rangle$ state, can be emulated fault-tolerantly by a two-qutrit Clifford+T unitary without ancillae, with a T-count of 12.*

Proof. The decomposition is as follows. Recall that each of the 4 $|2\rangle$ -controlled $X_{\pm 1}$ gates has a T-count of 3.

$$\begin{array}{c}
 \text{---} \textcircled{2} \text{---} \\
 \text{---} \boxed{X_{01}} \text{---}
 \end{array}
 =
 \begin{array}{c}
 \text{---} \boxed{X_{12}} \text{---} \textcircled{2} \text{---} \boxed{X_{-1}} \text{---} \textcircled{1} \text{---} \boxed{X_{+1}} \text{---} \textcircled{A} \text{---} \boxed{X_{12}} \text{---} \\
 \text{---} \boxed{X_{-1}} \text{---} \textcircled{1} \text{---} \boxed{X_{-1}} \text{---} \textcircled{1} \text{---} \boxed{X_{-1}} \text{---}
 \end{array}
 \quad (60)$$

□

Corollary 3. *By Equation (59), the qubit CCX gate can be emulated unitarily without ancillae using Clifford+T gates, with T-count 12.*

For the CCZ gate, from [79, Proposition 5.5]:

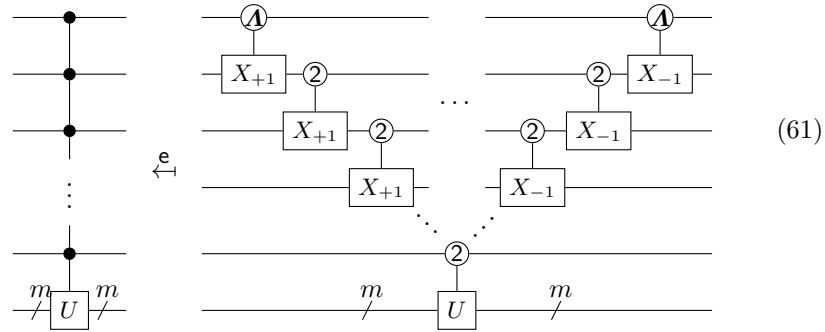
Proposition 5. *The qubit CCZ gate can be emulated unitarily without ancillae using Clifford+R gates, with R-count 3 and Clifford CX-count 5.*

Proof. Consider the qubit CCX gate emulation in Equation (59). If instead the controlled gate on the target is the $|2\rangle$ -controlled qubit Z gate in [79, Corollary 5.4], which has R-count 3 and Clifford CX-count 3, the emulated gate is the qubit CCZ gate. \square

The most straightforward way to generalize this to the qubit multiple-controlled Toffoli is the following linear gate count and linear depth decomposition:

Proposition 6. *The technique of emulating the qubit Toffoli can be generalized to n controls, and for any unitary U which can be $|2\rangle$ -controlled.*

Proof.



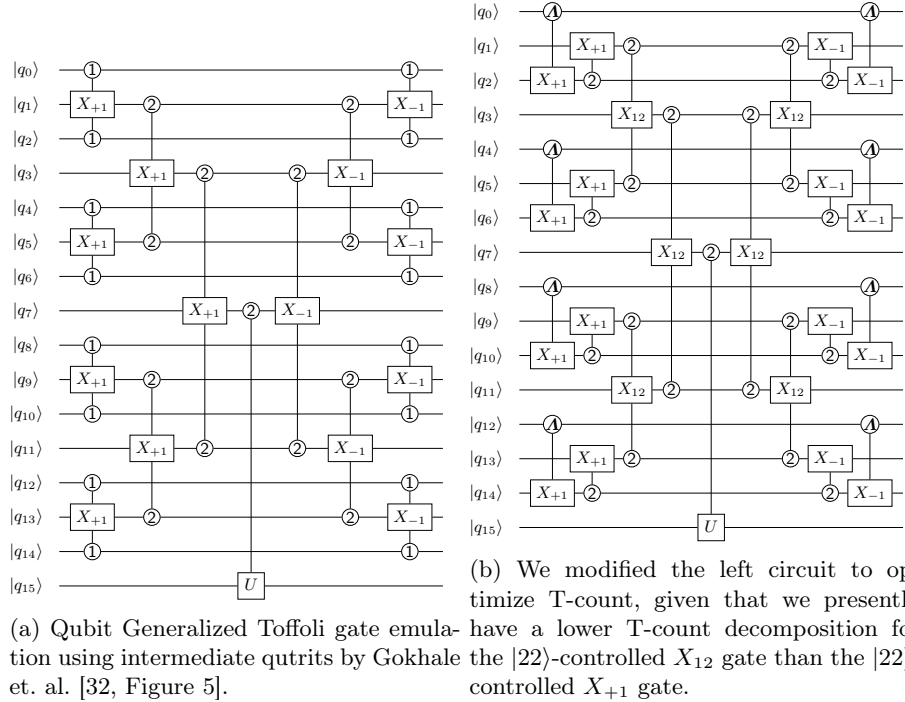
As each $|2\rangle$ -controlled $X_{\pm 1}$ gate is comprised of three qutrit T gates, the T-count is $6(n - 2)$ plus the cost of implementing the $|2\rangle$ -controlled unitary. \square

Corollary 4. *As the qubit Toffoli gate $|2\rangle$ -controlled qubit X gate can be constructed with T-count 12 according to Proposition 4, the qubit generalized Toffoli with n controls can be unitarily emulated without ancillae using qutrit Clifford+T gates, with T-count of exactly $6n$.*

This is an improvement over [7, Corollary 9], which emulates the qubit CC-NOT gate (i.e. $n = 3$) with T-count 18 using two clean ancillas, or T-count 21 using one clean ancilla.

In logarithmic depth, qubit multiple-controlled Toffoli gate can be built from qutrit Toffoli gates [5, 32]. Gokhale et. al. [32] leveraged the $|22\rangle$ -controlled gate to construct a qutrit emulation of the qubit Toffoli with n controls, with circuit depth logarithmic in n . We reprint their decomposition in Figure 3a. They cited the decomposition for the $|22\rangle$ -controlled X gates by Di and Wei, in terms of qubit Clifford+T gates pairwise between the three qutrit computational basis

states. As far as we know, a protocol to simultaneously error correct for these three gate sets has not been formulated.



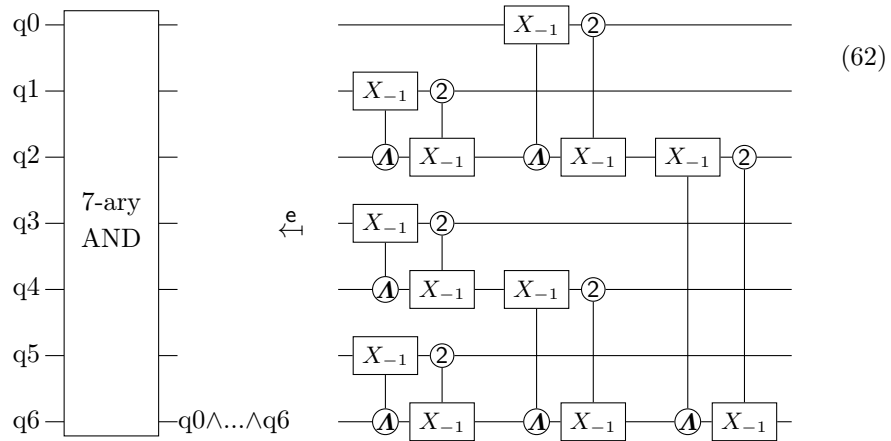
Using the decomposition for $|22\rangle$ -controlling any qutrit unitary V from [82, Lemma 1] to build $|22\rangle$ -controlled X_{12} in 51 T gates, we adapt their decomposition in Figure 3a to the qutrit Clifford+T gateset. We thereby achieve linear qutrit T-count for the qubit generalized Toffoli gate, whilst retaining the desirable properties of logarithmic circuit depth and no logical ancillae needed (i.e. only using those necessary for magic state injection). We find it to be more efficient in qutrit T-count to modify each of their $|22\rangle$ -controlled X_{+1} gates to $|22\rangle$ -controlled X_{12} gates, for a constant factor improvement in lowering the T-count. To further decrease the resource requirements, we note that all boundary (either the inputs or outputs are qubits) $|22\rangle$ -controlled gates in this decomposition are overconstrained; substituting them with our CCX_{+1} unitary decomposition in Equation (56) with T-count 3 suffices.

Despite this decomposition being linear in T-count, the coefficient of linearity is quite high, given that our decomposition for the $|22\rangle$ -controlled X_{12} gate has T-count 51. It is the first fault-tolerant decomposition for it and we have not yet attempted to optimize this, reason being that there is a far more efficient construction using the n -ary AND gate familiar from binary classical computing,

implemented on superconducting qutrits in [18], and resynthesized here in qutrit Clifford+T.

Proposition 7. *Consider the n -ary binary AND gate, which returns 1 iff all binary inputs are 1, and 0 otherwise. It can be emulated unitarily by Clifford+T gates without ancillae, in $\log(n)$ depth, with T-count $3n - 3$ and Clifford CX-count $4n - 4$.*

Proof. This follows from the equivalent well-known construction in classical reversible computation. The idea is to apply the T-count 3 emulation of the binary AND gate from Lemma 1 $n - 1$ times, as a binary tree structure. This generalizes to any positive integer n . The $n = 7$ case is shown below:



□

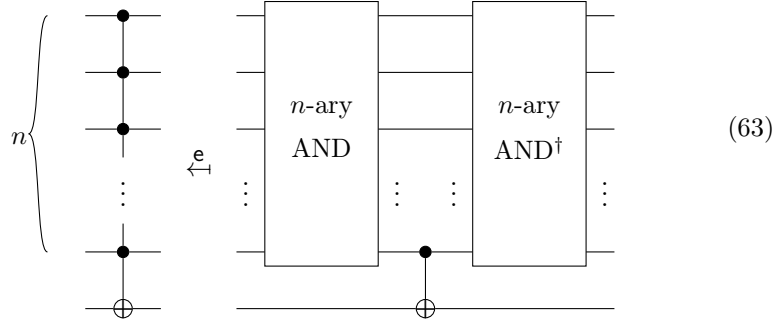
At first glance, it may seem that with the exception of the AND'd output, the other outputs can be disregarded. However, they are necessary for the gate as a whole to be unitary and thus reversible. At the end of this section, we will demonstrate the usefulness of being able to compute and uncompute the n -ary binary AND gate.

This means that the multiple-controlled qubit Toffoli admits the following decomposition when n -ary AND is available [18], for which we computed the T-count:

Theorem 1. *The qubit C^n X gate can be emulated unitarily without ancillae in qutrit Clifford+T gates in $O(\log(n))$ depth, with T-count exactly $6n$ and Clifford CX-count $8n$.*

Proof. First apply the n -ary binary AND gate emulation of Proposition 7 with T-count $3(n - 1)$ and Clifford CX-count $4(n - 1)$, where the bottommost output wire is the AND'd output. Then, we apply the qubit CX gate emulation of Lemma 4 controlled on the AND'd output, targeting the target of the C^n X gate, with T-count 6 and Clifford CX-count 8. Finally, we uncompute the n -ary

binary AND gate by applying its inverse, also with T-count $3(n-1)$ and Clifford CX-count $4(n-1)$.



The T-count totals exactly $6n$ and the Clifford CX-count totals exactly $8n$. \square

Corollary 5. *This construction can be generalized to gates of the form $C^n U$, controlled on $|1\rangle^{\otimes n}$ for qubit inputs, where U is any target unitary acting on m qudits for which a controlled version, for some type of control, can be built.*